ABSTRACT

MURRAY, IAN JAMES. Investigation of using Paper Microfluidic Techniques as a means of Improving Paper Spray Mass Spectrometry's Analytical Capabilities. (Under the direction of Drs. Michael Bereman & David Muddiman.)

Reducing analysis time and maximizing detection capability have long been goals in analytical chemistry. Many times, advancement of these aims have been technique specific with little crossover between fields. Yet in the last two decades two different techniques, miniaturized total chemical analysis systems (μTAS) and ambient ionization, have had significant advances around a common substrate, paper. Invented by R. Graham Cooks in 2010, paper spray ionization (PS) is a direct sampling ionization technique developed to quickly analyze complex biological mixtures without the need for timely sample preparation. While this technique has proven successful in detecting several compounds in complex biofluids, advances in improving the technique have been relatively limited to adding external functionalities to a fabricated paper substrate's cartridge. Therefore, prior paper-based technologies have been reexamined in order to advance paper spray by incorporating functionalities onto the paper itself. For over two decades microfluidic paper-based analytical devices (μPADs), the paper-based derivative of μTAS, have been created that are simplistic, diverse, and versatile in a host of fields. While research into coupled μTAS-MS systems have been conducted, equivalent μPAD-MS research is lacking. Herein, is presented both the characterization of several fundamental μPAD techniques incorporated onto the paper spray substrate and the devolvement of a simple 3-dimensional μPAD-PS device for rapid extraction, enrichment and detection of triazines in soil. This research provides the foundation and emphasizes the potential of inexpensively fabricated paper lab-on-a-chip devices coupled to mass spectrometry for in-field analysis.

Investigation of using Paper Microfluidic Techniques as a means of Improving Paper Spray Mass Spectrometry's Analytical Capabilities

by
Ian James Murray

A thesis submitted to the Graduate Faculty of
North Carolina State University
in partial fulfillment of the
requirements for the degree of
Masters of Science

Chemistry

Raleigh, North Carolina

2016

APPROVED BY:

_____	_____
Michael Bereman Committee Co-Chair	David Muddiman Committee Co-Chair
_____	_____
Glenn Walker	Edmond Bowden

DEDICATION

To Rachel, for all your loving support and help in pursing my goals. To my family, without your love and support I would not be the person I am today.

BIOGRAPHY

Ian James Murray was born in Bridgeport, West Virginia on October 30, 1991. Ian's parents are Roger and Mary Ann Murray. Ian grew up in Bridgeport, West Virginia and attended Bridgeport High School. Ian attended West Virginia University from 2010 to 2014 receiving his Bachelor of Science degree in Chemistry and minored in American History. While studying, Ian had the opportunity to work with the Governor's School for Math and Science and because of this experience was motived to continue his education into Chemistry to help expand the outreach of the sciences. Ian was greatly appreciative to have the opportunity in August 2014 to enter graduate school in the Department of Chemistry at North Carolina State University under the supervision of Dr. Michael Bereman. Dr. Bereman challenged him to purse the creation of new technologies and techniques to increase the versatility of paper spray mass spectrometry for the real time detection of potentially harmful compounds. Upon completion of the Master of Science degree in Chemistry, Ian will begin working at a Juris Doctor degree with the intent of working in the Intellectual Property field to protect fellow scientist's research.

ACKNOWLEDGMENTS

I would like to express appreciation for the help of those who helped bring this work to fruition. My family members provided moral support which was invaluable. I would like to thank my advisor Dr. Michael Bereman for many helpful conversations and feedback. I would like to thank committee members Drs. David Muddiman, Ed Bowden, and Glenn Walker for helpful feedback. Additionally I would like to thank Josh Beri and Gina Hilton for their support and friendship. Finally, I would like to thank North Carolina State University for funding this research.

TABLE OF CONTENTS

LIST OF TABLES

LIST OF FIGURES

CHAPTER 1 GENERAL INTRODUCION

1.1 Ambient Ionization

Mass spectrometry (MS) has become the premiere analytical tool for detection of compounds in complex matrixes due to its high sensitivity and unparalleled molecular specificity. This ability to analyze a vast set of compounds ranging from low (e.g., metabolites) to high molecular weight proteins, harkens to what J.J. Thomson felt the technique could accomplish: "I feel sure that there are many problems in chemistry, which could be solved with far greater ease by [Mass Spectrometry] than any other method."[3] Over the last two decades technology development around this technique has led to an exponential growth in its use and capabilities.

The first "contemporary revolution", personified by the work of 2002 Nobel Prize winners John Fenn and Koichi Tanaka, came as a result of trying to ionize high molecular weight macromolecules. Prior ionization techniques were largely limited to low molecular weight highly volatile species which significantly restricted the application of mass spectrometry to large biomolecules. The development of these techniques were simply revolutionary in their ability to ionize large biomolecules in a sensitive manner.

ESI, invent by John Fenn[4], is a liquid-phase "soft" ionization technique that produces multiply charged analytes after the application of a high DC voltage to a liquid conducting solution. At voltage onset a Taylor cone, producing a charged solvent mist, is formed at the end of a finely tapered capillary opening. The opening on many commercially available capillaries is on the range of 10 microns. Analyte ions are created via a combination of solvent

evaporation and Coulombic “explosions”. The resulting ions are then lifted into the gas phase and are sampled by the atmospheric interface of the mass spectrometer. ESI allowed for the coupling of separation techniques such as liquid chromatography and capillary electrophoresis to mass spectrometry, affording the separation of complex mixtures prior to mass analysis. Almost appearing simultaneously with ESI was matrix-assisted laser desorption ionization (MALDI). Coined by Hillenkamp and Karas[5], and advanced by Tanaka[6], MALDI uses an energy absorbing matrix, typically an organic acid for UV wavelengths, to assist in “soft” ionization. While the exact mechanism of ionization is hotly debated[7,8], recent research has

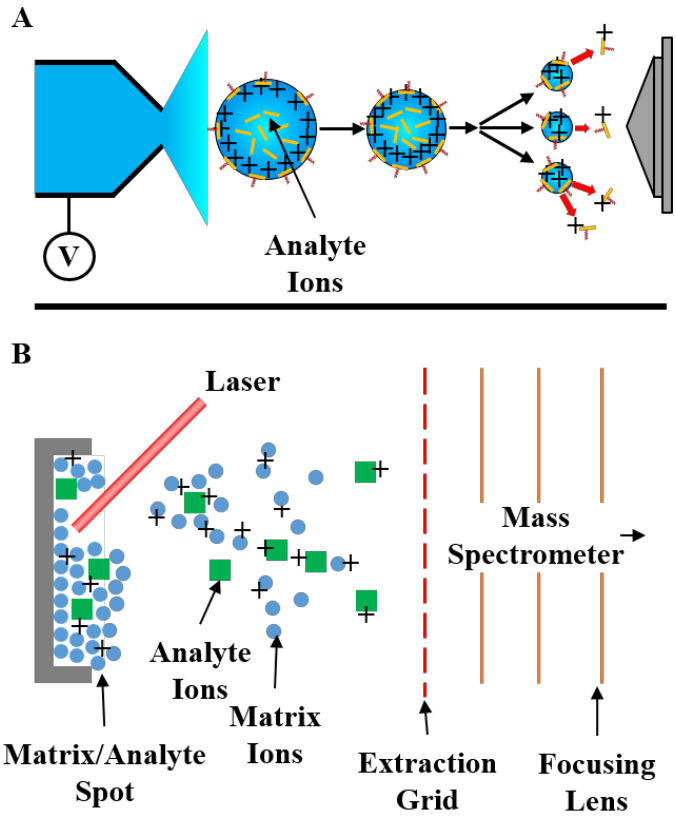

Figure 1.1: Ionization source schematics for **(A)** electrospray ionization and **(B)** matrix-assisted laser desorption ionization (MALDI).

theorized that thermal proton transfer after laser ablation of both the sample and matrix plays a significant role.[9] Simplified schematics for both ESI and MALDI can be seen in **Figure 1.1**. Although these two techniques differ in certain areas (e.g., MALDI is conducted under vacuum), their creation resulted in a tectonic shift in how ionization was both performed and thought about.

While these two techniques have led to the development of several new areas of research, significant limitations do exist. ESI requires significant sample preparation and MALDI requires a vacuum and a suitable matrix. Therefore, a push to analyze compounds in a more high throughout and native state was desired.

What some have called the "second contemporary revolution" of mass spectrometry was the development of ambient ionization mass spectrometry, or direct sampling mass spectrometry.[10] These techniques would allow for simpler and more rapid analysis of a sample due to, in large part, limited sample preparation. The first in this family of techniques was desorption electrospray ionization (DESI), created by Graham Cooks in 2004.[11] This

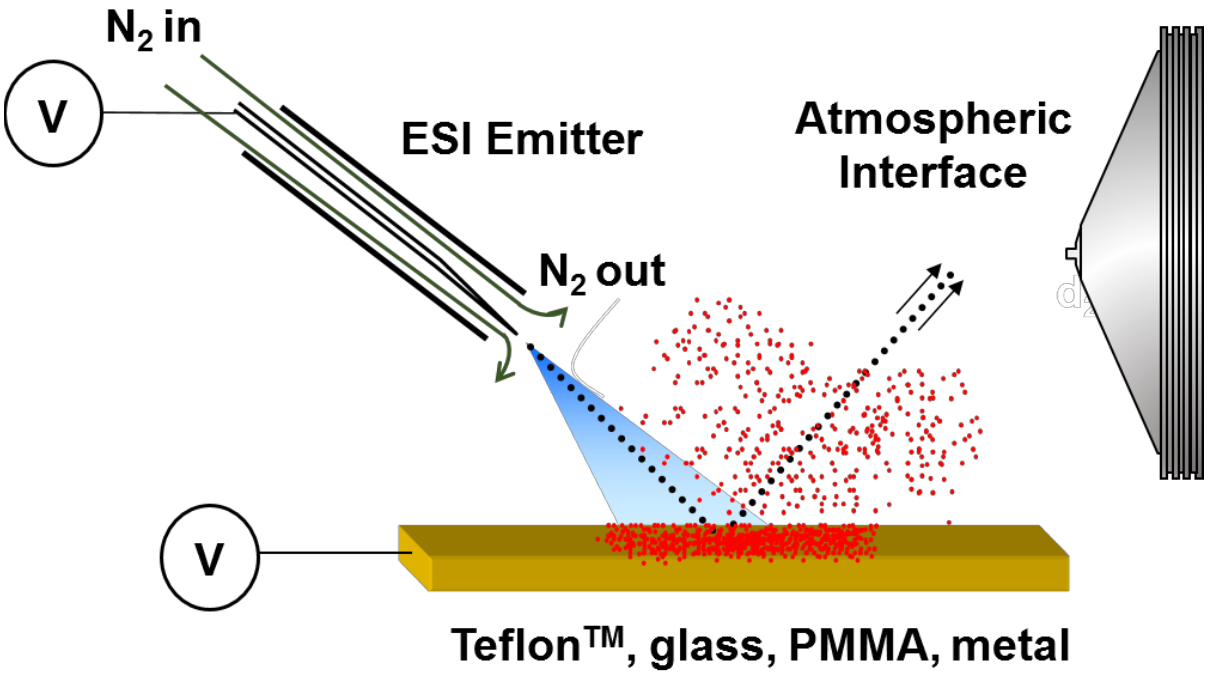

Figure 1.2: Diagram of a typical desorption electrospray ionization (DESI) setup.

technique combined electrospray ionization with the capability to analyze material deposited onto surfaces. In DESI, an electrospray mist is directed at a sample on a surface or in imaging studies the sample constitutes the surface. The charged mist droplets subsequently ricochet off the surface carrying desorbed analytes with them. These desorbed analytes are then ionized by their charged transporting droplet in an ESI-like manner and sampled by the atmospheric pressure interface of the mass spectrometer.[11] A diagram of the typical DESI setup can be seen in **Figure 1.2**. Over the next decade several more ambient ionization techniques were developed using a host of different materials and methods. Some of these techniques included: Direct analysis in real time (DART)[12], Atmospheric pressure solids analysis probe (ASAP)[13], and Matrix-assisted laser desorption electrospray ionization (MALDESI)[14] to name a few[15]. While all these techniques allowed for direct analysis of samples with limited to no sample

preparation, each technique had its own unique advantages and potential disadvantages in terms of both complexity and application. A relatively new ambient ionization technique, paper spray ionization, has garnered significant interest for its simplicity and utility.

1.2 Paper Spray Ionization

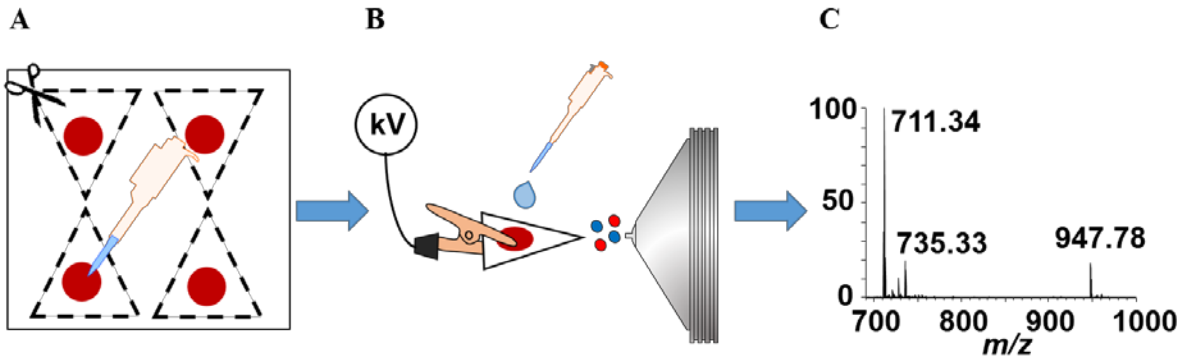

Figure 1.3: **(A)** Sample loading and cutting out of a typical paper spray triangle. **(B)** Application of spray solvent and voltage to create subsequent spray plume. **(C)** Resulting mass spectra.

Recently, analysis by mass spectrometry has been attempting to incorporate in-field analyses into its library of techniques. While miniaturization of the mass spectrometer's mass analyzer and detector have had their respective advances[16], finding an adequate ionization source was another task. An appropriate ionization source had to be easy-to-use, versatile, reproducible, and sensitive. During the rapid creation of ambient ionization sources, in which over 25 separate sources were created by 2009[17], many substrates were evaluated for potential use. One of these examined substrates was paper.

Paper has been used in analytical purposes for centuries.[18] In the 1940's, the work of Martin and Synge advanced the substrate as a useful separations medium[19,20]. More recently, Graham Cooks used paper as an ionizing substrate. This new direct analysis technique, called paper spray ionization (PS), provides an easy-to-use interface, limited sample preparation, low cost,

and ability to be coupled to miniaturized systems.[21,22] By loading the porous material with both a desired sample and a spray solvent mixture, a high voltage (>3.5kV) can be used to initiate a static electrospray.[23,24] An example workflow for a typical paper spray analysis can be seen in **Figure 1.3**. While PS has gained a reputation as an excellent sample substrate for analyzing a wide variety of compounds in blood spots[25-30], PS has also been used in the analysis of other complex biofluids and small molecules.[31-33] The technique is still ever advancing as seen in the number of publications released on the topic since its inception, as seen in **Figure 1.4**. Recently the technique has been commercialized by Prosolia under the trade name PaperSpray®.[34]

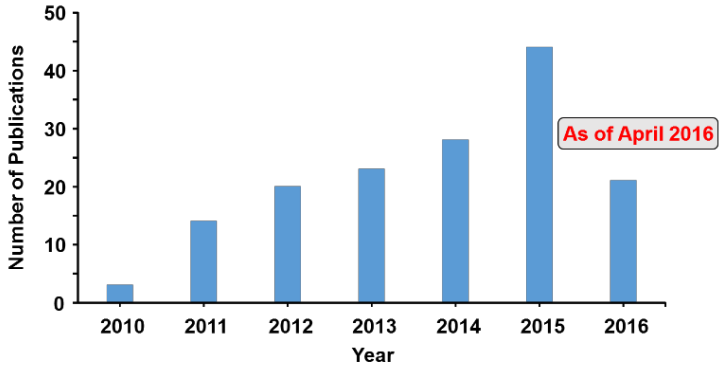

Figure 1.4: Number of publications about paper spray mass spectrometry as of April 2016.

Although PS has several advantages due to its simplicity, it still suffers from several drawbacks. PS notably has issues with ion suppression[35], poor extraction of the analyte[36,37], and limited analysis times due to spray solvent loss[23]. Yet since the technique's creation, there have been advances to overcome these limitations by applying both substrate alterations and external functionalizations. Carbon nanotubes and silica have been used to coat the paper and increase hydrophilicity[29,38] and physical additions to specially designed paper cartridges, such

as solid phase extraction columns[39] and continuous solvent addition sources[40], have been used to increase the techniques capabilities. These alterations and additions have been more successful at remediating the technique's inherent drawbacks than truly advancing the technique's analytical versatility. To both overcome many of PS's limitations and advance the technique's versatility, possible coupling to another paper-based technology, paper-based microfluidics, are being explored.

1.3 Paper-Based Microfluidics

While the study of fluidics has been around for centuries[41] microfluidics, commonly described as the manipulation of volumes between 10^{-6} and 10^{-18} liters, is a more recent field.[42] Microfluidics came about through a combination of necessity and technological capability.[42] The need for compact, versatile, and high throughput chemical analyses and the advancement of microfabrication processes pushed research forward in the early 70's and 80's.[42,43] In particular, the United States' Defense Advanced Research Projects Agency (DARPA) provided a significant boost to the field of complex and miniaturized chemical tests as a means to protect soldiers from potential biological warfare in the latter stages of the Cold War.[44] This work came into fruition in the early 90's with the creation of miniaturized total chemical analysis systems (μTAS). Initial μTAS chips, created by Manz and co-workers, were small silicon chips with several chemical manipulations integrated directly onto the chip.[45] Manz's intent with μTAS was to scale down several separations procedures and perform them all on the same device as to decrease both overall analysis time and experimenter experience demands.[46,47] These new devices proved to incredibility successful and in 1995 the number of

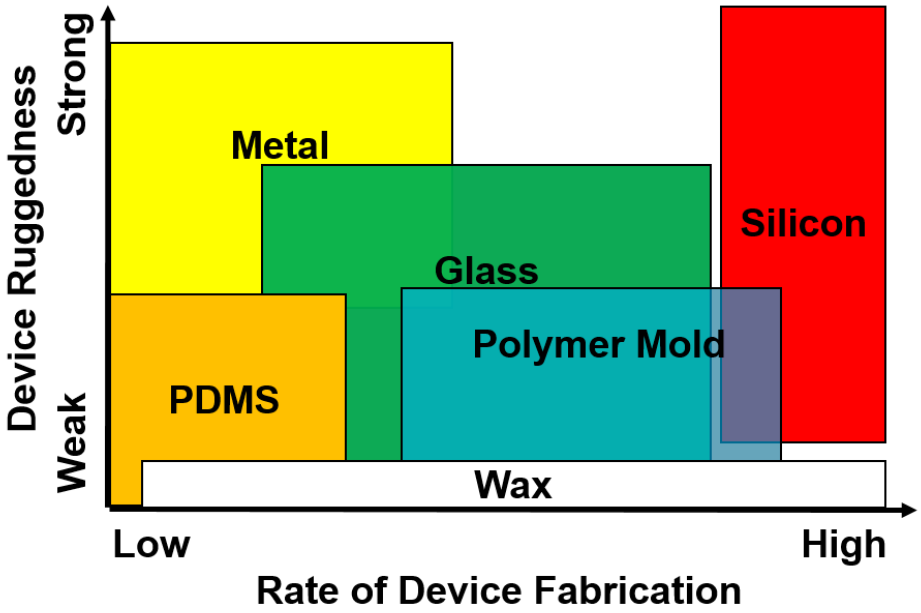

Figure 1.5: Listing of several materials used in μTAS fabrication plotted according to their described "ruggedness" and rate of device creation.

groups actively performing research this field exploded.[47] A particular field of inquiry during this time was in microfabrication and material selection. While much of the initial fabrication work came from the silicon microprocessor industry, in order to cover a broader range of chemical tests and applications new materials and techniques were required.[47] As seen in **Figure 1.5**, several new substrate materials were examined. Each material varied not only in its respective fabrication technique but also in both its ruggedness, resiliency to physical and chemical stressors, and rate of possible device fabrication. The result of this work was a diverse menagerie of devices with varying substrate materials, integrated functionalities, and detection methods. With the growth in device variety so too grew the variety of purposed applications. One of these areas of use was in-field health monitoring and for this type of device to succeed, devices need to be inexpensive, portable, and be quick and numerous to fabricate.[48] While

many µTAS succeed in the latter two requirements, cost was and still is a limiting factor for many µTAS devices[49]. A new kind of device was needed.

In 2007 Whitesides demonstrated the first paper-based microfluidic device, or µPADs, by imprinting photoresist into filter paper and forming both walls and separate derivatized assay zones.[48] These walls directed sample, being carried by capillary action, into the assay zones for colorimetric analysis.[48] Since this initial success several µTAS functionalizations have been incorporated on-substrate for µPADs usage.[49-52] This work has led to an expansion of inexpensive and easy to manufacture rapid diagnostic devices in numerous fields.[49] While these devices have changed the game, there is still one potential drawback. µPADs devices rely on colorimetric, fluorometric, or electrochemical detection methods[49], and while not necessarily an issue these detection methods do lack a degree of specificity and universality needed for high quality and accurate diagnostic devices[53].

Although µPADs parent technique, µTAS, has a history of coupling to the more desirable detection method of mass spectrometry (µTAS-MS)[54], this work has not translated into couplings between µPADs and mass spectrometry. But with the introduction of paper spray ionization (PS), possible µPAD coupling to mass spectrometry is now possible due to the common substrate material. This possible coupling is also advantageous as each technique offsets the others weaknesses. PS lacks on-substrate functionalizations that could assist in complex sample analysis and µPADs lack a highly selective and versatile detection method. Therefore, a coupled µPAD-MS device could potentially be the versatile, inexpensive, sensitive, and compact technique that is needed for future rapid and in-field diagnostic analysis.

1.4 Conclusions

As the world's population continues to grow exponentially, the demands for food and water will only increase. This demand for the bare essentials will lead many in developing countries, and the impoverished in most developed countries, to seek out any means to provide for themselves and their families. This pursuit for survival with both an increasing population and decreasing resources will potentially lead to increased rates of exposure to many harmful diseases and compounds.[55] Therefore, the detection and monitoring of these exposures will be vital for ensuring a healthy global public. Yet with a more mobile global public, these detection methods need to be in real-time, have comparable detection capabilities to established laboratory techniques, and be able to be used by a wide range of users. Research in developing these new devices and techniques are already underway and are being made of the simplest of all materials, paper.

Paper has recently been used in developing two powerful, yet separate, analytical techniques. Work in μTAS, also referenced to as Lab-on-a-Chip, have created easy to use all-in-one chips capable of a host of complex chemical manipulations.[56-58] While much of the research into μTAS has been translated into paper-based versions, μPADs, these devices rely on colorimetric, fluorometric, or electrochemical detection methods.[49] Although these detection methods are powerful in their own right, more universal and selective methods are required for an ever expanding list of potential hazards. A better suited detection method is mass spectrometry, and recently a paper-based mass spectrometry technique has been developed.[21] Paper Spray (PS) is an easy to use technique which unlike μPADs, has lacked

significant increases in its capabilities since its basic iteration. Coupled µPAD-PS technologies could potentially bridge the gaps between each techniques drawbacks and provide a sensitive, all-in-one, easy-to-use device for in-field monitoring of harmful compounds. Yet, many questions need to be addressed for this reality can occur.

In Chapter 2, fundamental aspects of coupling paper-based microfluidics techniques and paper spray mass spectrometry are addressed. Chapter 3 outlines the potential of using simple microfluidic barriers to increase the sensitivity of native paper spray. This chapter also addresses the potential of integrating more complex 2-dimensional physical manipulations onto the paper substrate. Chapter 4 characterizes the coupling of 3D paper-based microfluidics to paper spray mass spectrometry and demonstrates the potential of a simple 3D-µPAD-PS device. The Appendix describes a Design of Experiments optimization of our basic paper spray protocol and solvent compatibility testing of a prototype 3D printed paper spray cartridge.

CHAPTER 2 BASICS OF COUPLING MICROFLUIDICS TO PAPER SPRAY MASS SPECTROMETRY

2.1 Introduction

Paper has had useful analytical purposes for centuries[18], and while many believe that the modern rise of paper as a useable and versatile substrate started with Martin's work in 1942-44[19,20], an impregnated paper microfluidic device had already been around for a couple of years. In 1937 paraffin wax was being patterned onto paper to create uniform wells for qualitative spot testing.[59] After the initial success using paraffin wells, in 1949 a paraffin channel was produced on paper in an attempt to demonstrate preferred elution of dye mixtures.[60] Although this work proved successful, the required fabrication techniques proved to be too complex for the time and did not receive industrial attention.[49] Because of this lack of industrial interest, financial support was not available and much of the academic work around paper-based technologies in the following decades revolved around much simpler lateral flow and dip stick assays. These assays included the initial at-home glucose monitoring[61] and pregnancy testing[62], yet these tests are more closely related to immunological tests rather than traditional microfluidic devices. These assays primarily consisted of an impregnated band of antibodies[62-64] within the paper that upon wetting would give a "yes" or "no" colorimetric response. While many modern microfluidics devices use similar detection methods for real time analysis, modern devices have far more functionality and have placed a greater emphasis on the fluid dynamics and manipulation.

It wasn't until the early 1990's that both fabrication technologies advanced, many of which were borrowed from the technologies used to create microchips for computers, and cost decreased enough that a renewed interest in microfluidic devices occurred. During this time the concept of "miniaturized total chemical analysis systems" (μTAS), coined by Manz and co-workers during their work with silicon chips capable of several chemical manipulations[45], began to gain prominence.[46] These μTAS devices, constructed from chemically inert materials like ceramic, glass, and silicon[57], proved to be capable of a series of chemical and flow manipulations. This new class of devices are what is now understood to be modern microfluidic devices. Yet these devices relied on fluorescence or electrochemical detection methods which, although sensitive, do not scale well with miniaturization.[54] As research into μTAS flourished, several novel detection systems in fields ranging from health sciences[65] to environmental monitoring[66] were created. Yet, it was the continued advancement of the micro and nanoscale fabrication methods that would prove most valuable for the eventual coupling of μTAS to more sensitive and miniaturized detection systems, such as mass spectrometry (MS).

Electrospray ionization (ESI), a form of atmospheric ionization in which a voltage is applied to a liquid to create an aerosol consisting of ionized analytes[67], appeared to be the most likely candidate for possible μTAS-MS coupling. The issue with this coupling though proved to be that early ESI instrumentation, invented six years before μTAS by John Fenn, was simply not compatible. In 1996, Mann and coworkers designed "nanospray" ionization (nanoESI)[68], an improvement on the initial ESI technique which both greatly reduced the overall size and increased detectable signal. Mann demonstrated that there were several advantages from

decreasing the inner diameter of the emitter: a decrease in the required spray voltage, closer placement of the emitter tip to the mass spectrometer, decreased sample consumption, decreased flow rate, and increased analyte ion yield compared to normal ESI.[68] The stringent fabrication requirements of nanoESI, fine tipped emitters with micron diameters, could easily be reproduced on chips using established μTAS techniques, thereby making the techniques compatible. This capability, alongside the multiple functionality and inexpensiveness of chips, made coupling of nanoESI emitters and μTAS possible, practical, and useful.

A coupled μTAS-nanoESI device implements electrospray ionization in one of three general ways. These approaches include spraying directly from an edge of a chip, implanting a silica-emitter into the edge of the chip, and directly integrating or fabricating an emitter into the chips.[54] Although each system has its own advantages and setbacks, the approaches all suffer from roughly the same drawbacks of substrate brittleness and poor ease-of-use. During the rise of μTAS-nanoESI coupled microfluidic chips, paper was largely ignored as a possible μTAS substrate. In 2007 Whitesides and co-workers showed that simple patterned paper could incorporate many of the same capabilities as other μTAS chips and was of far greater ease to use and create.[48] In a short time paper as a μTAS substrate, called microfluidic paper-based analytical devices (μPADs), became a burgeoning field of study and began being used in a plethora of applications.[49] Around the same time as the development of μPADs, another paper-based technique was being created. Paper-spray ionization (PS), invented by Graham Cooks, is an electrospray ionization derivative using a finely cut paper tip as the ESI emitter.[21] Much like μPAD technologies, PS found many applications particularly in the fields of drug

monitoring and biofluid analysis.[27,30,32,69,70] Yet, unlike the coupling that happened between μTAS and nanoESI technologies, there has not been such a coupling between μPADs and PS.

Herein, we examine the fundamentals of coupling μPAD techniques to the PS setup. In normal PS, the paper substrate is unaltered aside from the addition of the analyte and spray solvent. By adding functionalization to the paper's surface, in the form of hydrophobic barriers, there could be unforeseen consequences. Of the multitude of possible barrier materials currently being tested, we focused on two of the more common materials: SU-8 photoresist and solid wax ink.[71] We demonstrate that the background signal, use of organic solvents, and fabrication requirements are not detrimental to possible μPAD-PS coupling.

2.2 Material and Methods

Materials

Rhodamine 6G dye (R6G) was obtained from Sigma-Aldrich (St. Louis, MO). High performance liquid chromatography (HPLC) grade methanol, isopropyl alcohol, and water were from Burdick and Jackson (Muskegon, MI). Whatman Grade 1 filter paper sheets of were purchased from GE Healthcare Bio-Sciences (Pittsburgh, PA). Negative epoxy resist, SU-8 3010, was purchased from Microchem Corp (Newton, MA). All mass analyses were performed using a Q Exactive Plus Orbitrap mass spectrometer (Thermo Scientific, Bremen, Germany).

Fabrication of Hydrophobic Barriers

Barrier designs were drawn using Abode Illustrator (v.CS6). All designs were exported as PDF files for printing and can be found in the **Appendix** (**Figure A.5**). A commercially

available Xerox Phaser 8580 ColorQube printer was used to print wax onto the surface of the filter paper. Wax designs were printed directly onto letter size, 215mm x 280mm, cut sheets of filter paper with no adjustments to the printer's factory settings. Printed wax designs were covered with aluminum foil and heated on a digital hot plate at approximately 110 ^{o}C for 2 minutes. Melted designs were allowed to cool to room temperature on a cooling rack and stored until use. Designs intended for use with photoresist were sent to DTPRESS Commercial Printing (Greensboro, NC) to be printed as transparent film photomasks. Photoresist barrier fabrication took place in a clean room located in the Biomedical Engineering Department (NC State University, Raleigh, NC). Small pieces of Grade 1 filter paper, 60 mm x 60 mm, were manually coated on both sides with a thin layer of SU-8 3010 photoresist and placed on a hotplate at 130 ^{o}C for 15 minutes. The SU-8 impregnated paper was allowed to completely cool and placed between a piece of black construction paper and the desired transparent film photomask. The resulting "sandwich" was exposed to a 9.7mW/cm^3 ultra-violet (UV)-lamp for 100 seconds. The patterned paper was heated again at 130 ^{o}C for 5 minutes to complete cross-linking of the epoxy. The patterned paper was thoroughly rinsed in acetone and isopropanol until all visible unpolymerized photoresist was removed. Further cleaning of the paper was performed in an oxygen plasma cleaner at low power to remove any remaining organic solvents.

Background Signal Testing

The capillary temperature on the Q Exactive Plus Orbitrap mass spectrometer was set to 325 ^{o}C and the tube lens voltage was set to 60 kV. A voltage of 4.3 kV was applied by an

attached copper alligator clip to initiate paper spray ionization. Triangular pieces of paper of equivalent surface areas with either no barriers, wax-printed barriers, or photoresist barriers (**Figures A.5A** and **A.5B** respectively) were loaded with 50 µl of methanol/water (1:1, v/v) and analyzed until solvent was depleted.

Resolution after Melting and Solvent Containment

Twelve wax-printed wells varying in printed wall width from 0.05 mm to 1 mm were fabricated on a single piece of filter paper (**Figure A.5C**). Well widths were measured before and after heating to determine the amount of expansion from melting. After cooling, each well was loaded with 50 µl of dilute R6G in 1:1 water/MeOH for visualization purposes. Signs of visible leakage served as indicators of barrier failure.

Organic Swell Determination

Six sets of wax-printed parallel lines, with a width of 1.25 mm (**Figure A.5D**), were fabricated and loaded with 50 µl aliquots of a mixture with varying methanol concentration (0, 20, 40, 60, 80, 100%). A Celestron Deluxe Handheld Digital Microscope (Torrance, CA) was used to measure the wall swell caused by the percentage of organic solvent present. High resolution images were taken with a Zeiss Light Microscope at the Analytical Instrumentation Facility (NC State University, Raleigh, NC).

2.3 Results and Discussion

2.3.1 Fabrication

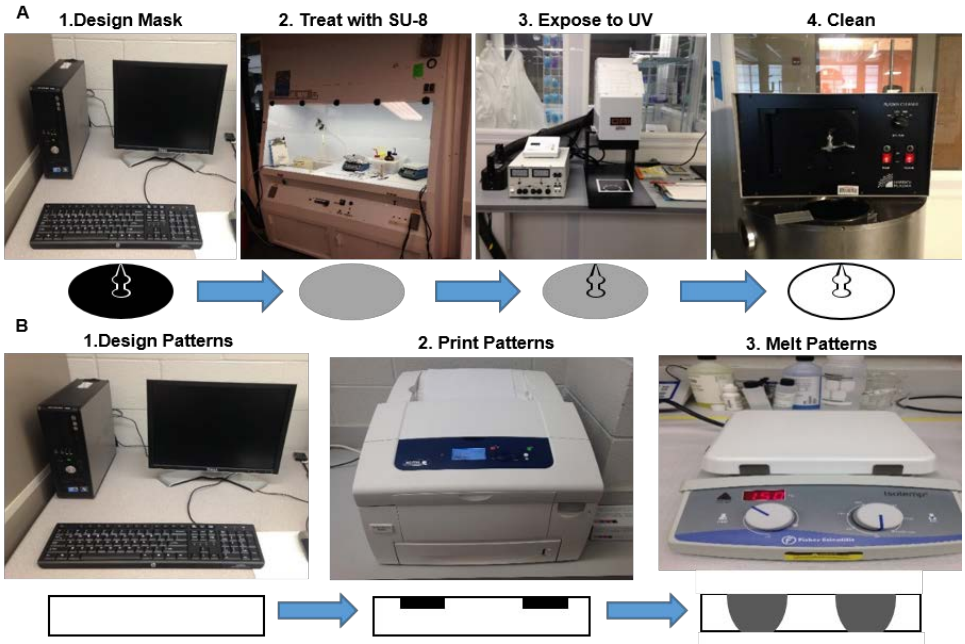

Figure 2.1: Schematic representations of workflows for **(A)** photoresist and **(B)** wax-printed designs.

Figure 2.1 shows the workflows for the fabrication of both the photoresist and wax-printed paper spray designs. There are several reported barrier materials and fabrication techniques[72-75], but the photoresist and wax-printed barrier materials represent two of the more commonly reported methods for paper-based microfluidic devices.[49,71,76] Although photoresist presents a host of advantages to other fabrication techniques, such as well-defined stable barriers[77] and complete penetration of the paper, barrier creation with photoresist is more cumbersome than wax-printed barriers due to facility requirements, material costs, and mask creation.[78,79] Photoresist barrier creation protocols, including “rapid” methods, present greater

time and cost constraints in comparison to wax-printing.[76,79-81] These issues can make fabrication with photoresist more prohibitive for some laboratories on a practicality level.

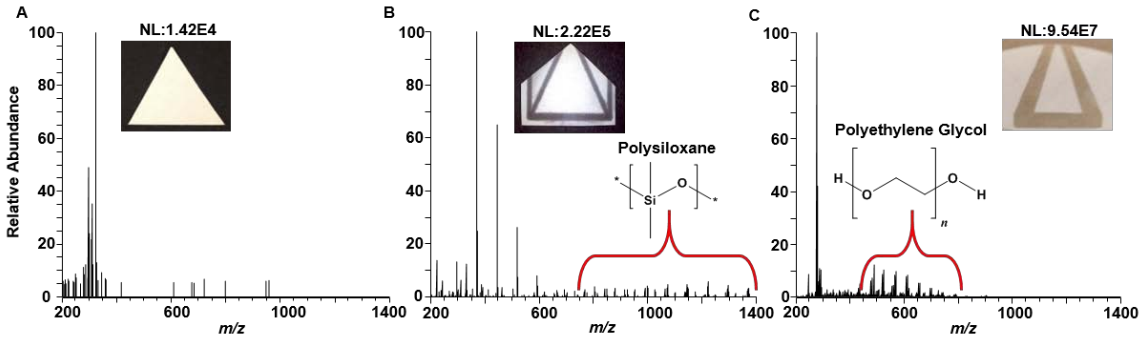

Figure 2.2: Background spectra for each of the three microfluidic barriers types while spraying with 50ul 50:50 Water:MeOH. **(A)** No Barrier **(B)** Wax and **(C)** Photoresist SU-8

A concern with various microfluidic devices when coupled to electrospray ionization mass spectrometry (ESI-MS), is the potential for a large chemical background detected from the ionizing substrate.[53,82,83] To investigate potential residual "scum" from uncrosslinked photoresist and the spreading of wax, photolithography and wax-printing background signals were analyzed and compared to unaltered paper.[81,84] Shown in **Figure 2.2**, both wax-printed and photoresist altered paper had higher levels of background signal in comparison to unaltered filter paper. Wax-printed barrier's background signal was 1 order-of-magnitude higher than unaltered paper, with several detectable background signals between *m/z* 900 and 1400, and several of those signals had a spacing of 74.0185. This repeat unit is indicative of polysiloxane species, a common component in waxes.[85] Photoresist's background signal was 3 orders-of-magnitude higher than unaltered paper. Similar to wax, photoresist had a set of repeating background signals. Between *m/z* 400 and 800, there were signals with a repeat unit of 44.0261, indicative of polyethylene glycol (PEG).[85] Significant background signal is a concern and can

be detrimental to analytical performance as it can suppress signal from low abundant ions. Due to paper's fibrous construction and the total coating method required in photoresist fabrication, is it probable that leftover uncrosslinked photoresist remains trapped in the paper, despite several rounds of thorough washing and plasma cleaning. Although more vigorous wash methods[86] aside from the ones performed herein could reduce background signal using the photoresist method, wax-printed paper devices were found to be simple, have limited background contamination, and do not require additional cleaning. Therefore, wax-printed barriers were used for all subsequent experiments described.

2.3.2 Resolution after Melting and Solvent Containment

Unlike photolithography, in which the epoxy completely penetrates the paper, wax printers print the wax on top of the paper with only minimal penetration into the paper. Therefore, the wax must be heated in order to spread vertically to the opposite side for wax-printed devices to provide complete liquid containment. Standard filter paper is produced by pressing together cellulosic fibers into a material with a naturally anisotropic fiber structure.[49,79,81] **Figure 2.3** illustrates the anisotropic structure.

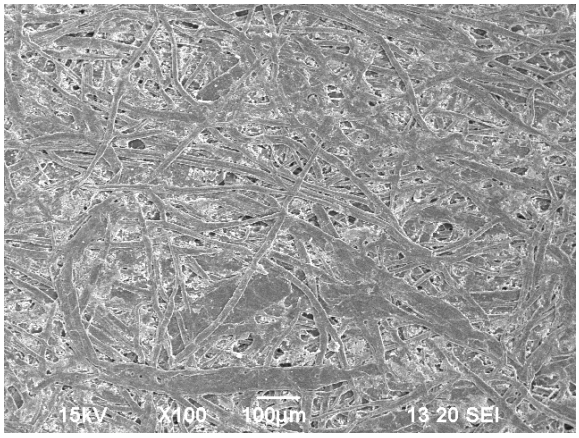

Figure 2.3: Image of Whatman No. 4 Filter paper under an electron scanning microscope at 100X magnification.[1]

The pressing process causes the fibers to be directed in the horizontal plane more often than the vertical plane of the paper, leading to the lateral spreading of fluids in paper being more rapid than vertical spreading.[79,81] Because of this, final barrier widths are wider than the initial printed size after wax heating. The difference between initial printing size and final size due to melting can be seen in **Figure 2.4A**. This widening caused by the heating of wax yielded a highly correlated linear relationship over a range of printed widths, as seen in **Figure 2.4B**. Our results roughly match those of Carrilho and coworkers, showing that reproducible and predictable fabrication is possible while using inherently variable wax .[81]

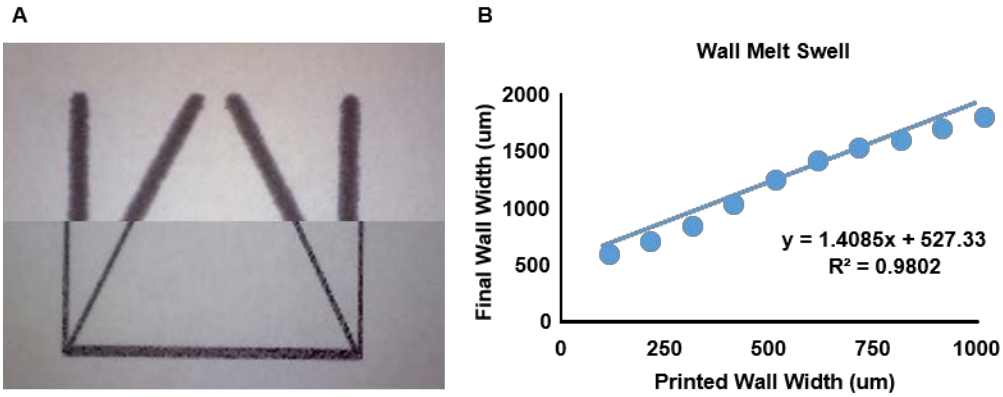

Figure 2.4: **(A)** Before and after of melting wax printed lines on filter paper. **(B)** Wall swell due to melting at various printed widths.

Although the widths of wax-printed barriers are more significantly variable than photolithography, they are still a common method used for fluid control on paper.[81,87] Yet due to the physical limitations in the amount of wax printed, minimum initial wax-printed widths must be determined to both ensure complete vertical spreading and to minimize for lateral spreading. Wells were printed with varying initial wax amounts, seen as the different wall widths in **Figure 2.5**, to determine the minimum initial wax required to form a complete seal post-melting. Walls with 0.3 mm initial printed widths were found to be the minimum width,

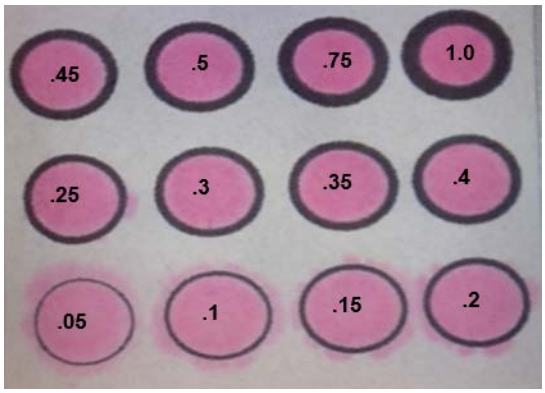

Figure 2.5: Walls of varying thicknesses printed wax thickness from 0.05 mm to 1 mm (0.05 mm increments between .05 mm and .5 mm and .25 mm increments between .5mm and 1 mm) were created and loaded with equal volumes of dilute R6G dye in 50/50 Water/Methanol solution to determine minimal containment thickness.

and therefore the minimum amount of wax needed, to ensure complete sealing of the paper for fluid containment on a consistent (100%, n = 10) basis. Walls with 0.25 mm initial printed widths did completely seal the paper but at a sporadic rate (45%, n = 10). Walls with an initial barrier thickness of 0.4 mm were used throughout subsequent experiments to ensure containment. It is important to note that these results are only for Whatman Grade 1 filter paper, with a depth of ~180 µm, and different brands would need to be tested individually.

2.3.3 Organic Swell Determination

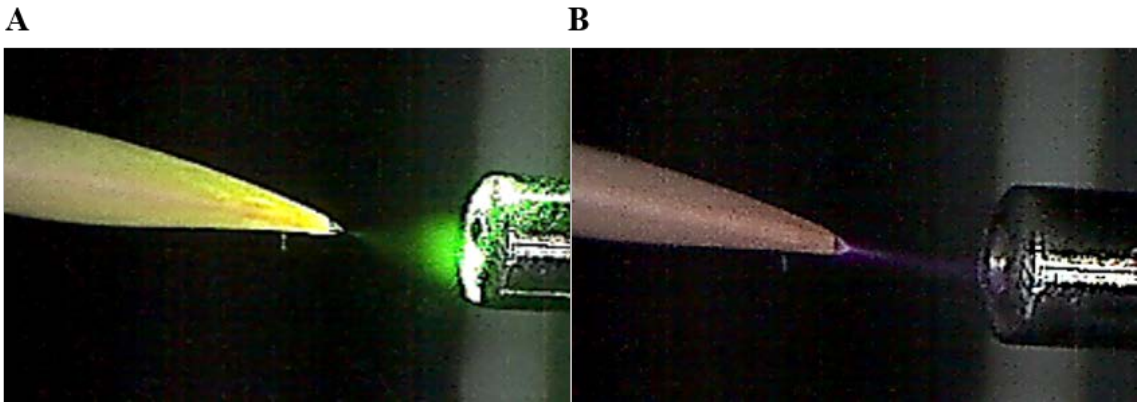

Figure 2.6: (A) Spray jets and spray cone created under "Rich" organic conditions. There are three spray jets present. **(B)** Spray jet and spray cone created under "Poor" organic conditions. There is a single jet created.

Useful paper spray ionization is dependent on several factors including the angle of the spraying tip and the applied spray voltage.[88] Of particular interest for effective coupling of microfluidic techniques is their compatibility with commonly used spray solvents, such as acetonitrile and methanol. Paper spray occurs in one of two modes depending on the amount of spray solvent present and the organic composition. Spray solvents "Rich" in volatile organics (≥50% of total volume) and plentiful in amount, allow for fast solvent flows and formation of multiple cone jet sprays, as seen in **Figure 2.6A**, that are essential for optimal

ionization and detection with paper spray ionization.[23,89] Spray solvents that are depleted or are mostly aqueous, also called “Poor” conditions, are known to produce coronal discharges, as seen in **Figure 2.6B**.[23] This can be useful for analyzing particular compounds such as aromatic hydrocarbons, but usually results in signal intensity loss.[23]

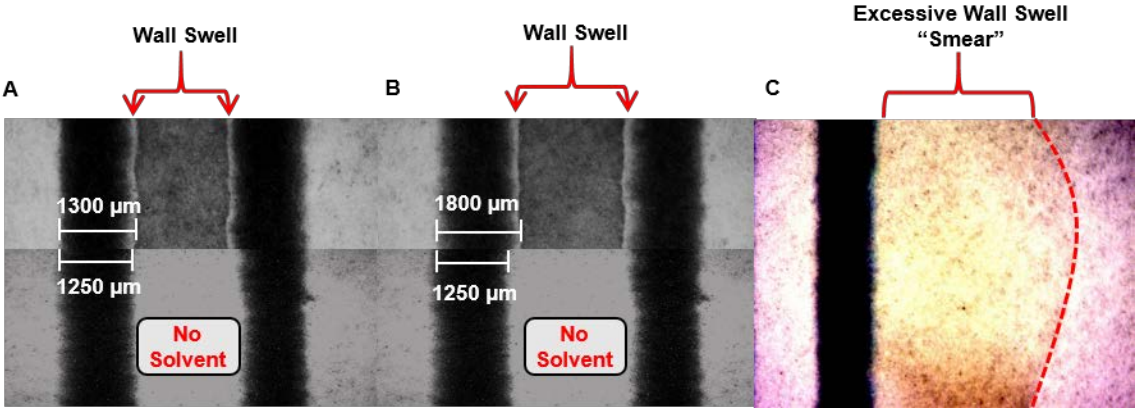

Figure 2.7: Magnified images of wax walls subjected to: **(A)** 0% methanol. Images of wax walls not exposed to solvent are included for visual comparison. The black ink used to color the wax did not appear to spread. **(B)** 60% methanol. Images of wax walls not exposed to solvent are included for visual comparison. The black ink used to color the wax did not appear to spread itself. **(C)** 100% methanol. 100% methanol resulted in no swelling but rather a smearing of wax and ink. Red line was included on the outermost boarder of smearing for visualization purposes. Images were altered to show greater contrast.

Unlike photoresist, organic solvents are noted to lack compatibility with wax-printed barriers due to their ability to wick through the wax causing swelling[71,81] and detrimental loss of analyte. To determine organic solvent’s effect on wax barriers resolution, barrier swell was measured as seen in **Figure 2.7A-C**. Spray solvents with different percent volumes of methanol were added to wax barriers with equal width and final swells were determined by measuring the width of the new visible width.

Spray solvents with organic compositions between 0 and 80% total volume showed a strong linear relationship ($R^2 = 0.9897$) with total wall swell as shown in **Figure 2.8**. Visually, there was no significant amount of "wicked" spray solvent on the opposite side of the barrier. Therefore, leakage due to wicking appeared to be negligible. Although spray solvents consisting of <80% organic by volume results in minimal wall swelling due to solvent wicking, spray solvents consisting of pure organics led to a complete smearing, indicated by the discoloration between the outside of the wax barriers and the dashed red line, of the wax on the paper as seen in **Figure 2.7C**. Thus, a 50:50 (v:v) organic/water spray solution was used in all experiments to reduce wall swelling, avoid leakage, and maintain optimal paper spray stability.

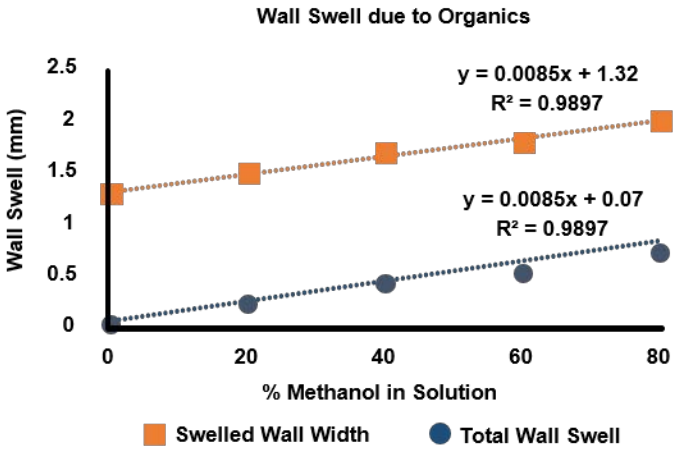

Figure 2.8: Parallel lines of wax printed lines (Initial widths of 1.25mm) were subjected to solutions of varying methanol composition. Swelled Wall Width is the visible width observed after exposure to an organic solution. Total Wall Swell is the difference between initial and swelled wall widths.

2.4 Conclusions

Of the several dozen barrier materials currently used in paper-based microfluidic devices, both solid ink wax and SU-8 photoresist were evaluated in this study for their potential for coupling to mass spectrometry via paper spray ionization. Photoresist, an organic resin that forms highly defined channels upon exposure to UV-light, was found to be unfavorable for possible coupling with mass spectrometers due to both its high level of background signal when using common paper-spray spray solvents and its laborious fabrication procedures. Wax on the other hand proved to be a more ideal barrier material. Wax had a background much lower than photoresist, within 1 order-of-magnitude to unaltered paper, and its fabrication was of greater ease. This large discrepancy in background signal levels between barrier materials is most likely due to the inability to completely remove photoresist resin from the fibrous paper substrate and not the stability of the material itself. The author notes that when creating barriers with wax, steps have to be taken to understand the effects of melting and organics on both the final resolutions of the initial printed substrates and their ability to contain liquids. Although wax lacks the fine resolution capable by photoresist, it does not prohibit it from being a robust barrier material and coupling potential to mass spectrometers. Future experiments will explore the possibility of using wax barriers to conduct on-paper chemical reactions and increase the sensitivity of paper spray.

CHAPTER 3 IMPROVING ANALYTICAL PERFORMANCE

3.1 Introduction

Within the last decade, paper spray mass spectrometry has grown from an analytical novelty to a commercially available high throughput technique.[34,90] Paper spray's growth has been the result of its incredible ease-of-use and particular utility in analyzing complex biofluids.[21,31,35] Paper spray mass spectrometry is a direct analysis technique, which means that most of its analyses are performed in a "Point-and-Shoot" method. A "Point-and-Shoot" method is one where no intentional chemical or physical manipulations are imposed upon a sample at any point prior to or during analysis.[21,23,28,30,33,37,88,91,92] Complex samples are loaded onto the paper substrate and analyzed directly on the mass spectrometer. While there are exceptions, these examples are few in number and are normally limited to performing preexisting simple organic reactions on the paper's surface prior to applying a spray voltage.[93-96] Although this "Point-and-Shoot" method has been shown to be sufficient for analyses where targeted analytes are relatively high in abundance[26,27,97], the technique has several inherent limitations which inhibit the technique's sensitivity and robustness.

Paper spray ionization has notable issues with ion suppression from complex matrixes[35], poor extraction of analyte from either complex matrixes or the paper's fibrous structure[36,37], and limited analysis times due to spray solvent loss[23]. While there has been some research into directly studying these inherent limitations[35], there has been a greater amount of research into overcoming these limitations and thereby improving paper spray's performance. The research into increasing paper spray's performance can broadly be categorized into two

regimes: addition of an external device and substrate functionalization. External devices have been used to create continuous solvent application[40,98] or filter detrimental debris[39] before loading the sample onto paper. This is normally done by either a 3-dimensional printed cartridge[39,40,98] or a pre-treatment microfluidic chip.[99,100] While a typical paper spray method may only have an analysis time of 1 minute[21], devices intended to create continuous solvent application increase analysis times to 4 to 10 minutes.[40,98] Devices with filtration features, such as an integrated solid phase extraction column, showed increased limits of detection for several tested analytes, but these results were sporadic and shown to be compound specific.[39] Although these external devices did show some successes in improving performance, they also add a layer of technical complexity to the technique. 3D printing and microchip fabrication, although becoming less expensive[101], are both a financial and technical barrier for most labs. This increase in complexity is at odds with the fundamental idea of paper spray mass spectrometry, which is ease-of-use. Another more simplistic option to improve the technique's sensitivity is to completely modify the paper substrate. Two substances that have been examined as paper substrate modifiers are carbon nanotubes[102] and silica[29]. While these substrate modifiers showed an improvement in paper spray detection capabilities, they each also have inherent flaws. Carbon nanotubes are a known toxicant and can cause pulmonary disease[103], and silica makes paper brittle and hard to handle. Completely coating the substrate can also limit the possibility of incorporating other functionalities onto the substrate's surface. Another possible avenue of research into improving paper spray mass spectrometry's performance while

limiting both unnecessary complexity and substrate alteration, is by coupling existing paper-based microfluidic techniques to the ionizing paper substrate.

Miniaturized total chemical analysis systems (μTAS) and microfluidic paper-based analytical devices (μPADs) work on a "sample-in/answer-out" method.[56] That is, after loading the sample for testing a clear colorimetric, fluorometric, or electrochemical signal will indicate a binary result of "yes" or "no".[57,64,74,104,105] These detection methods, although sensitive and specific for their particular analysis, pale in comparison to mass spectrometry's near universal approach for detection.[53] The more important feature of μPADs is the host of developed substrate functionalities for μPADs.[74,104] These functionalities, which affect only a small area of the substrate, allow for the possibility of several chemical and physical manipulations both on and within the substrates. The functionalities are incredibly easy to design and fabricate, allowing for quick customizability depending on the desired test requirements. Herein, we will investigate the utility of coupling two of the most common microfluidic functionalities to the paper substrate in order to improve the analytical figures of merit of paper spray mass spectrometry.

Paper spray ionization has been noted as having a low recovery rate. Only a limited amount of analyte can be extracted by the spray solvent, therefore any source of analyte loss must be reduced or eliminated.[29,36] Yang and coworkers demonstrated that fluid transport in paper spray is controlled by a combination of capillary action and bulk solvent movement.[88] Electrophoretic flow was shown to be non-significant.[88] These two transport methods present possible sources of loss from both the natural diffusion of analytes within the paper and the

dispersion of the spray solvent. Prior work in two-dimensional paper fluid transport has shown that solvent fronts expand radially at equal rates in all directions.[106] This presents a significant problem for paper spray mass spectrometry on two fronts. As the analyte disperses radially, the amount of analyte near the tip emitter decreases significantly. Yang and coworkers showed that analyte concentrations will be roughly equal at each of the emitter tips present in a common triangular paper-spray devices if normal spreading, capillary action, is allowed.[88] This equates to up to two-thirds of extracted analyte material moving away from the emitting tip. Although this spreading could be useful in theory for analytical replication, it is detrimental to the overall performance of paper spray. Another issue with spreading is the loss of spray solvent. Common spray solvents consist of mostly volatile organics. Therefore as the spray solvent spreads, its surface area increases, and in turn increases the rate of evaporation. With less spray solvent present there will be both decreased extracted analyte and decreased analysis time. By using the simplest of µPADs functionalities, hydrophobic channels, the spreading of both the analyte and spray solvent can be restricted and therefore potentially decrease analyte loss, increase detectable signal time, and increase sensitivity.[107]

These hydrophobic channels also present an opportunity to explore the effects of flow rate restriction on paper spray by constricting the emitter tip channel width. Considering that the mechanisms of paper spray and electrospray ionization are analogous[23,108] and the sensitivity of ESI is inversely proportional to the flow rate, lower flow rates may be another mechanism that yields increased ion abundances.[68,109-111] Therefore, hydrophobic channels could improve the sensitivity of paper spray in two distinct manners.

Another microfluidic functionality of particular interest for coupling to paper spray, is on-substrate mixing. The ability to mix micro and nanoliter volumes of solutions could immensely improve the sensitivity of paper spray mass spectrometry. The mixing of solutions lends to the possibility of derivatization and other desirable organic reactions where lendable, which can improve the sensitivity of paper spray. Analyte derivatization has been used for decades[112-114] to increase ion abundance by electrospray ionization. Thus, such designs could be used to achieve improved ion abundance by paper spray where the targeted analyte is lendable to derivatization. The practice of performing organic reactions on paper spray's surface to increase ion abundance, called reactive paper spray, has also been used for several years[93-95,115] and peptide derivatization is bound to be a future area of interest as there have been a growing number of peptide analyses via paper spray in the last few years.[108,116,117]

Mixing in microfluidic devices falls into two regimes, active or passive, in which either external energy or special configurations are used to facilitate mixing.[118] Although active mixing is possible in paper by a variety of energy sources[119-121], they present a layer of unnecessary complexity and run counter to paper spray's ideal of ease-of-use. On the other hand, passive mixers rely on the manipulation of the fluid's flow to thereby increase the contact time between the mixing species.[122,123] This manipulation of flow and contact time can be easily achieved by using hydrophobic channels to direct reacting mixtures towards each other and then a collection receptacle. Furthermore, there exists a large body of work in the field of passive microfluidic mixing.[118] From this body of work, extensive research into the optimization and fabrication of passive flow designs[122-124] can be reexamined, repurposed, and

eventually coupled to the paper substrate. For these reasons, the coupling of a passive mixer into the ionizing substrate could be a beneficial addition to the substrate.

Herein, we examine the effectiveness of coupling two common µPAD techniques, hydrophobic channels and on-substrate mixing, to paper spray's ionizing substrate in attempts to increase the techniques sensitivity. Paper spray mass spectrometry suffers from inherent limitations; such, as ion suppression[35] and poor extraction[36,37], which inhibits both its use in a wide range of applications and its overall performance. By adding application specific hydrophobic barriers, many of these limitations can be significantly limited and other advantageous features can be seamlessly incorporated. We demonstrate that the coupling of these two techniques to the paper substrate can increase the versatility and performance of the technique.

3.2 Materials and Methods

Materials

Atrazine, iodoacetamide (IAM), propazine, and rhodamine 6G dye (R6G) were obtained from Sigma-Aldrich (St. Louis, MO). High performance liquid chromatography (HPLC) grade methanol and water was purchased from Burdick and Jackson (Muskegon, MI). The sequence from human hemoglobin (GTFATLSELHCDK), which contains a free cysteine residue (Cys^{93}), was synthesized and purchased from Thermo Fisher Scientific GmbH (Ulm, Germany). Whatman grade 1 filter paper sheets of were purchased from GE Healthcare Bio-Sciences (Pittsburgh, PA). Fluorescence imaging was performed on a Bio-Rad PharosFX

system (Hercules, CA). All mass analyses were performed using a Q Exactive Plus Orbitrap mass spectrometer (Thermo Scientific, Bremen, Germany).

Concentration Effect

Triangular pieces of paper, with and without wax-printed barriers, were fabricated as shown in **Figure A.5E**, and 10 µl of a 100 µM R6G solution were pipetted in the middle of the emitter area and allowed to dry completely. The triangles were then loaded with 50 µl of methanol/water (1:1, v/v) and analyzed. Triangles were imaged before and after analysis with a Bio-Rad PharosFX system to visualize compound spread within the filter paper.

Flow Constriction

Two designs with wax-printed barriers of varying emitter widths, were fabricated **(Figure A.5E and A.5F)**, and 10 µl of a 100 µM R6G solution were pipetted in the middle of the emitter area and allowed to dry completely. The triangles were then loaded with 50 µl of methanol/water (1:1, v/v) and analyzed for 5 minutes. Each design was tested in triplicate.

Water Monitoring Test

Two designs, one of unaltered paper and one with wax-printed barriers **(Figure A.5E)**, were fabricated and were spotted with a 5 µl aliquot of (1:1, v:v) residential tap water and atrazine or propazine with concentrations ranging from 10 µM to 250 nM. Each spot was allowed to dry at ambient temperature for approximately 10 minutes. Samples were then loaded with 50 µl of methanol/water (1:1, v/v) and tandem mass spectrometry (MS/MS) was performed on either the protonated atrazine parent ion (*m/z* 216) or the protonated propazine

parent ion (*m/z* 230). The primary fragment ion (*m/z* 174 or 188 respectively) was isolated and used to compare each design's sensitivity. Results were recorded for one minute.

Mixing Reactions

A wax-printed design specifically fabricated for mixing was created and fabricated **(Figure A.5G)**. 20 µl of a 10 µM solution of hemoglobin peptide was simultaneously loaded into one well, while 20 µl of a 50 µM solution of iodoacetamide was added to the other well. The two solutions were allowed adequate time to completely mix and fill the end triangular receptacle. The triangles were allowed to dry before being cut out and analyzed.

3.3 Results and Discussion

3.3.1 Concentration Effect

Figures 3.1A and **B** illustrates two pieces of paper, each having equivalent working surface areas, loaded with equal amounts of the fluorescent dye and spray solvent. The integrated intensity of the extracted ion chromatogram, from **Figure 3.1C**, was on average 5.5-fold higher ($p < 0.05$) for barrier-printed paper compared to unaltered paper. It was hypothesized that by controlling for analyte and spray solvent spreading via hydrophobic barriers, the signal reproducibility of paper spray mass spectrometry could be improved. By restricting the spreading, all analyte movement is directed towards only one possible spraying tip. Therefore under equivalent testing conditions, detected signals should be highly reproducible. However, it was found that the improvement in variance of repeated analyses ($n = 5$) of the dye was only marginally significant (2-way f-test, $p = 0.089$).

The fluorescence images **(Figure 3.1A-B)** provide further evidence of the effects of capillary flow and bulk solvent restriction. After spray solvent deposition, unaltered paper (**Figure 3.1A**) showed a fairly uniform low concentration distribution of the analyte throughout the whole piece of paper. Barrier-printed paper (**Figure 3.1B**) showed a more concentrated portion of the analyte, indicated by the red "spot", in the channel leading to the emitter tip.

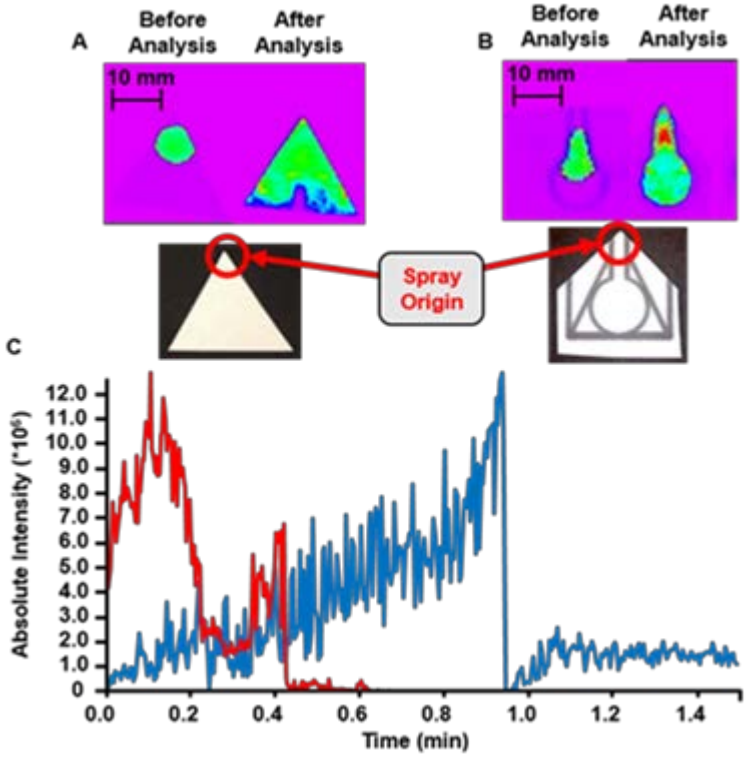

Figure 3.1: Images of **(A)** Untreated paper and **(B)** Wax barrier paper. Spread of R6G dye is shown before and after paper-spray analysis using fluorescence spectroscopy. Blue and green represents areas of relatively low dye concentration while red represents areas of relatively high dye concentration. **(C)** Extracted ion chromatograms of Rhodamine 6G dye for (Red) unaltered paper and (Blue) wax barrier paper.

This method shows that by using hydrophobic barriers, a one-dimensional transport can be used to effectively control capillary action and bulk solvent paths, and limit solution dilution from unwanted spreading.

In combination with a concentration effect, it was hypothesized that the restricted designs may also decrease the static flow rate in paper spray and therefore increase ion yield. As mentioned before, the mechanisms of paper spray and electrospray ionization are analogous.[23,108] According to work done by Mann, a relationship exists between the emitted droplet radius and the flowrate (V_f^2), fluid density (ρ), and surface tension (γ) as seen in **Equation 1**.[125] This equation can effectively be reduced to a relationship between emitted droplet radius and flow rate, as seen in **Equation 2**.

Equation 1: $$\boldsymbol{r_{emitted} \propto (\rho V_f^2 \gamma)^{1/3}}$$

Equation 2: $$\boldsymbol{r_{emitted} \propto V_f^{2/3}}$$

Therefore, as the channel to the emitting tip is restricted, bulk solvent movement is reduced and effectively lowering the flow rate. The lower flow rate in turn creates smaller droplets which, according to prior work in electrospray ionization, increase ionization efficiency and sensetivity.[68,125,126] This relationship between flow rate, droplet size, and sensitivity is further reinforced by work demonstrating that the sensitivity of ESI is inversely proportional to the flow rate.[68,109-111]

To further examine the effects of constricting flow on analysis time and signal abundance, two wax designs of varying emitter widths were examined. The first design was similar to the previous experiment and the 2nd design used a significantly restricted emitter

channel **(Figure 3.2A-B)**. The final widths of the designs were 3 and 1 millimeters respectively.

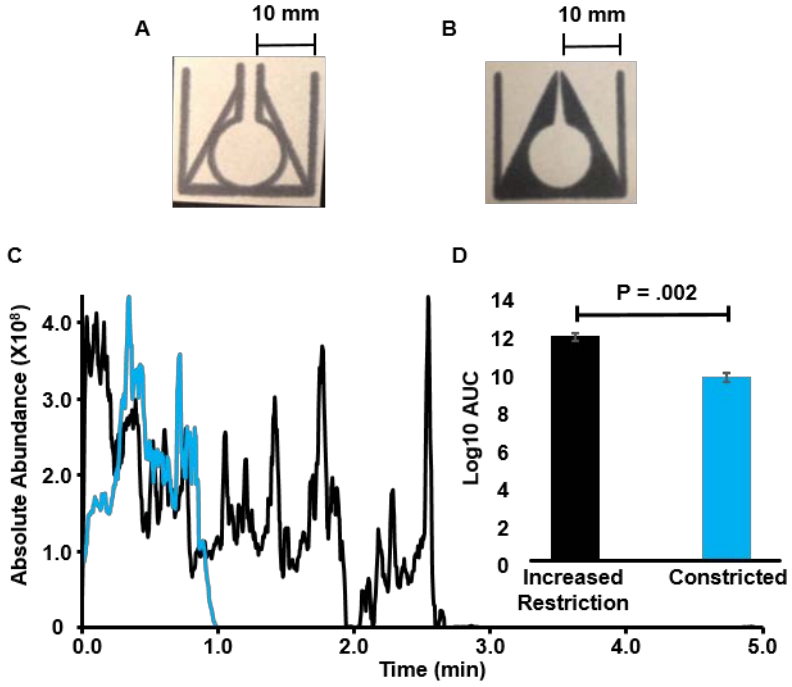

Figure 3.2: Images of tested paper designs **(A)** constricted and **(B)** Increasingly restrictive design. **(C)** Extracted ion chromatographs of R6G dye for constricted (Blue) and increasingly restrictive design (Black) designs. **(D)** Bar graphs of the Log10 area under the curve (AUC) and standard errors for each design. P-value between groups are also included.

Equal amounts of R6G dye were deposited on the two designs and analyzed in triplicate. **Figure 3.2C** displays a representative overlay of the extracted ion chromatograms using the two different designs. A direct relationship between emitter channel restriction and analysis time is apparent. Wax constricted paper **(Figure 3.2A)** on average offered a minute of consistent detectable signal, while the increasingly restricted wax design **(Figure 3.2B)** offered 2-fold extended analysis time. Pairwise comparisons between the two designs (n = 3) using a Welch's t-test confirmed that the more restricted design yielded significantly higher ion

abundances ($p < 0.05$). As a result, the mechanisms for increased ion abundance using wax patterned paper for paper spray mass spectrometry are likely due to both a concentration effect and lower flow rates leading to longer analysis times. The restricted designs should increase the sensitivity of paper spray based analytical assays. To provide further evidence for this hypothesis we analyzed the pesticides atrazine and propazine spiked into residential tap water.

It should be noted that although the increasingly restricted design offered both greater analysis time and ion abundances, the fine tip was less robust due to clogging during both the melting of the wax and sample analysis. However, with optimization of these designs could prove beneficial for the analysis of low abundant species.

3.3.2 Measurement of Pesticides Spiked into Water

A potential application of paper spray is the measurement of pesticides and other small molecules that are present in our environment and can affect human health.[37,97,127,128] Traditionally, pesticide analyses have been measured by GC-MS/MS and, more recently, by LC-MS/MS.[129,130] Unfortunately these techniques require laborious sample preparation and are not conducive for real-time analysis. Paper spray mass spectrometry could provide a solution for these more strenuous practices and yield both increased usability and expedited detections.[37,97,131]

Sample collection could be done in-field by wiping surfaces or depositing small water samples directly onto the paper surface and analysis could be performed with a miniaturized mass spectrometer. In a setup like this, hundreds of samples could be analyzed in a day. With the potential of paper spray as an in-field monitoring technique, improving the performance of the technique is paramount for both qualitative and quantitative measurements

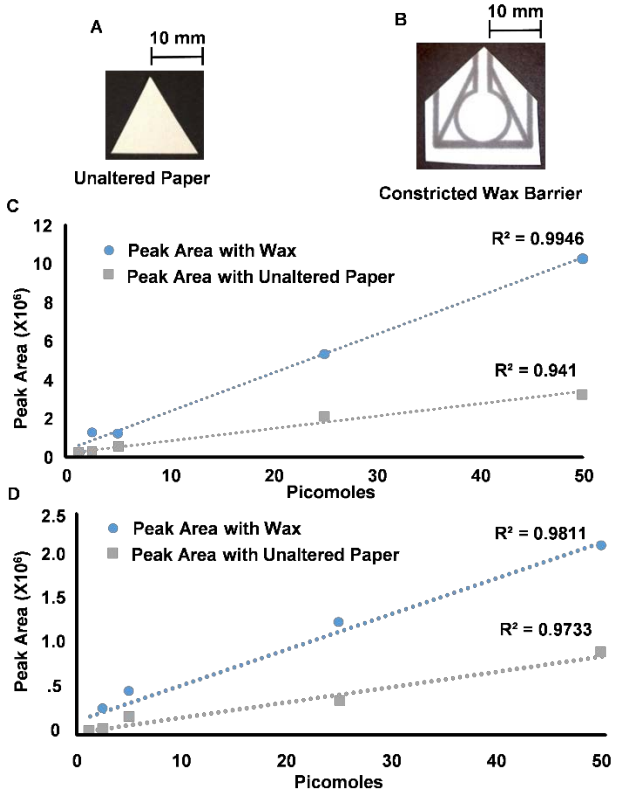

Figure 3.3: **(A-B)** Images of tested paper designs. **(C-D)** Peak areas of the atrazine fragment ion (*m/z* 174) and propazine fragment ion (*m/z* 188) respectively, in tap water at various loading amounts on the two tested designs. Linear regression and correlation coefficients are included for both.

Two designs were compared, as seen in **Figures 3.3A** and **B**, to measure either dilute atrazine or propazine spiked into residential tap water. The structures of the pesticides included in this study and their principle MS/MS fragmentation are reported in **Table 3.1**. Pesticides were spiked into tap water and spotted onto the paper (50 picomoles to 1250 femtomoles). The tested concentrations are within the U.S. Environmental Protection Agency's (USEPA) limits for triazines for several crop and commodities, as seen in **Table 3.2**.[132] It should also be noted that the lower range of tested concentrations match USEPA health advisory limits in drinking water for both seven year and single day exposure of 50 ppb and 100 ppb respectively.[133] Atrazine (*m/z* 216) was isolated, fragmented, and the primary fragment ion (*m/z* 174) was used for quantification. Detection of atrazine in tap water was discovered to be highly linear using both the wax ($R^2 = 0.9946$, $p < 0.002$) and unaltered designs ($R^2 = 0.941$, $p < 0.01$). Propazine (*m/z* 230) was isolated, fragmented, and one of the two primary fragment ions (*m/z* 188) was used for quantification. Detection of propazine in tap water was discovered to be highly linear using both the wax ($R^2 = 0.9811$, $p < 0.002$) and unaltered designs ($R^2 = 0.9733$, $p < 0.002$). The sensitivity (i.e. slopes) of the assays were compared using analysis of covariance (ANCOVA) and it was found that the restricted flow design yielded significantly higher sensitivity of both pesticides ($p < 0.002$). Thus, wax restriction should prove beneficial for analysis of low abundant analytes.

Table 3.1: Pesticides, and their respective information, involved in the analysis. Red arrows indicate location of fragmentation during MS/MS analysis. With both compounds this is a loss of propylene (-42 Da) from the isopropylamino side chain.

Pesticide	Nominal monoisotopic mass	$[M + H]^+$ transition	Principal fragmentation
Atrazine	215	216(*m/z* 216 → 174)	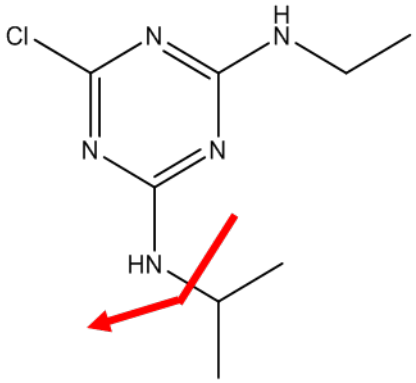
Propazine	229	230(*m/z* 230 → 188)	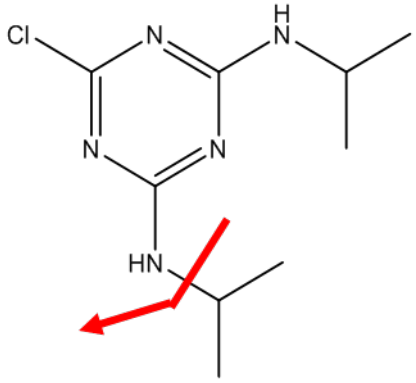

Table 3.2: Commodities and their respective USEPA triazine limits.

Commodity	Parts per Billion
Cattle, fat	20
Cattle, meat	20
Corn, sweet, kernel plus cob with husks removed	200
Grass, hay	4000
Milk	20
Sugarcane, cane	200
Wheat, grain	100
Wheat, hay	5000

3.3.3 Mixing

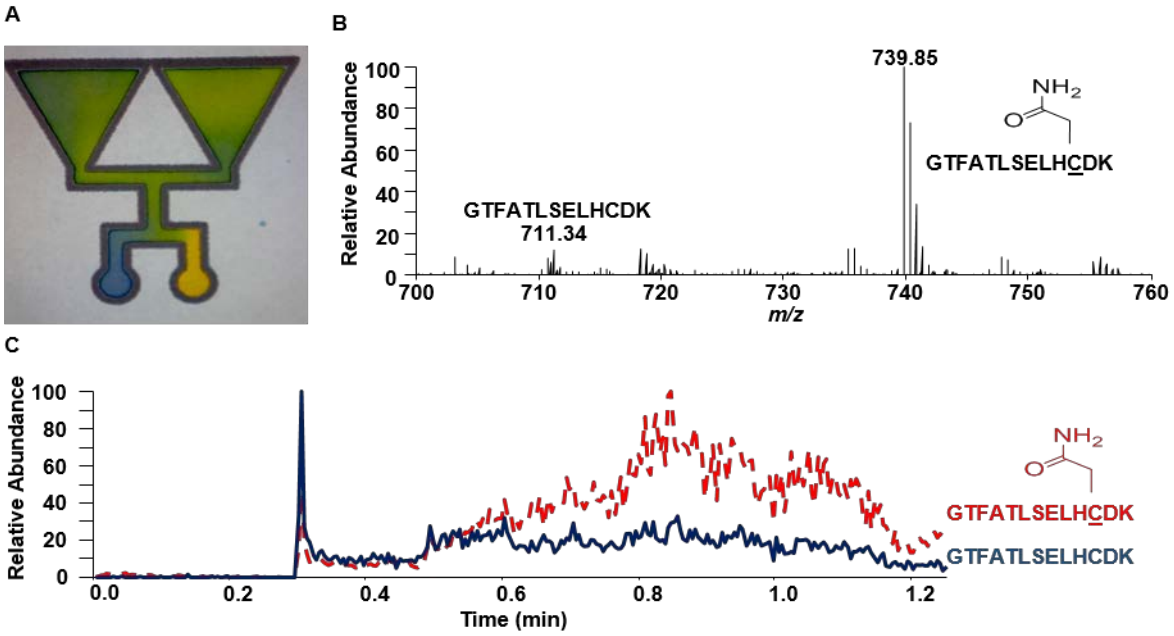

Figure 3.4: **(A)** Optical representation of the mixing of two solutions in a wax printer design with food coloring. **(B)** PS-MS spectra of a hemoglobin peptide with iodoacetamide and their respective peaks labeled. **(C)** Extracted ion chromatograms of both unadducted hemoglobin peptide (Blue) and carbamidomethylated hemoglobin peptide (Red).

As seen in **Figure 3.4A**, we used a simple T-junction passive design to increase simplicity in handling and use. In order for the device to have both sufficient mixing and be rapid (< 2 minutes), both the channel length and final reservoir designs had to be optimized.

By using hydrophobic barriers, the capillary flow can be simplified into one dimension and can be expressed by the Washburn equation (**Equation 1**), where L is the distance of the traveled by the solvent front, t is time, D is the pore diameter, γ is the surface tension and μ is the viscosity.[134]

Equation 3: $$L^2 = \frac{\gamma D t}{4\mu}$$

By assuming γ, D, and μ are constant, Washburn-like flow can therefore be effectively reduced to a relationship between distance and time (**Equation 2**). This shows that the capillary flow decreases over time and therefore long channel lengths result in impractical mixing times.

Equation 4: $$L \approx \sqrt{t}$$

Several channel lengths were tested (data not shown) until the time between sample addition and final reservoir filling was roughly two minutes. Capillary flow in triangular shapes with various cut angles have been previously studied.[106] A 60^{o} entrance was used in the final design to ensure quick filling of the final reservoir.

Herein an example of mixing is demonstrated via the alkylation of the hemoglobin peptide that contains a free cysteine (GTFATLSELHCDK, *m/z* 711). This peptide is of interest in the field of adductomics due to the high abundance of hemoglobin in blood and the reactivity of the free cysteine which essentially acts as a "sink" to reactive species.[135] The peptide was allowed to passively mix with iodoacetamide, an alkylating reagent, in order to achieve desired

peptide adduct. After mixing and mass analysis, the alkylated peptide (GTFATLSELHCDK, *m/z* 739) was the most prominent peak. As seen in **Figure 3.4B**, the unadducted peptide was detected but with a significantly weaker signal. Extracted ion chromatograms for both the unadducted and adducted are included in **Figure 3.4C** to compare relative abundances of each ion. The adducted peptide was detected at 4 times greater intensity than the unadducted peptide. These results demonstrate that relatively effective mixing can occur purely by passive mixing from wax-printed barriers.

3.4 Conclusions

Paper spray mass spectrometry is a growing technique for quick collection-to-answer analyses. Yet due to the several inherent limitations of the technique, its detection of low abundant species is poor. Therefore, techniques to mitigate these limitations must be explored if paper spray is to gain wide spread use. Herein, the characterization of two microfluidics techniques coupled to paper spray mass spectrometry were explored in attempts to increase its detection capabilities.

Wax-printed channels significantly increased ($p < 0.05$) the sensitivity of detection of two pesticides in paper spray ionization in comparison to unaltered paper. These channels restricted unwanted radial and bulk solvent flow away from the ionizing tip and therefore increased the amount of extracted analyte available for detection. This reduction in unwanted spreading also resulted in an increase in total analysis time. These results were repeated using a real world example by detecting pesticides spiked into residential water. In both pesticide cases, atrazine and propazine, there was a significant ($p < .02$) increase in sensitivity between

wax-printed barriers and unaltered paper. In a follow-up experiment, wax-printed barriers were also used to reduce the flow rate by restricting the size of the emitter channel. This reduction in the emitter channel width, and therefore flow rate, yielded a significant increase ($p < 0.05$) in sensitivity over the earlier used wax-printed barriers. These results provide more evidence linking the spray mechanisms of nanoESI and paper spray ionization. Although the more restricted emitter design proved to be less robust, it presents a possible area for continued research.

Utilizing both basic microfluidic principles of fluid movement and common proteomic derivatization techniques, mixing within the paper's fibrous matrix was attempted. Using the Washburn equation to predict capillary flow, channels were designed such that the total time between sample addition and end receptacle filling would be approximately 2 minutes. A hemoglobin peptide with a free cysteine (GTFATLSELHCDK, *m/z* 711) was mixed with a common alkylating reagent in order to detect the adduced peptide (GTFATLSELHCDK, *m/z* 739). Initial results showed that successful mixing was capable within the fibrous matrix. Although complete mixing was not detected, the adducted peptide was the predominate signal during the analysis. Future experiments will explore the possibility of using 3D microfluidic techniques to increase the functionality of paper spray in attempts to create a portable dual detection paper-based device.

3.5 Ongoing and Future Work

3.5.1 Chaotic Advection

Simple passive mixing between a hemoglobin peptide and iodoacetamide proved to be successful, as noted by the predominate presence of the adducted peptide peak in **Figure 3.4B**, but the mixing was not complete. Detectable amounts of the unadducted peptide remained and although this is not detrimental to the device's overall performance, it should be reduced if possible. Therefore, further research is proposed in order to examine the effects of slight alterations to the mixing design in order to increase contact time between reacting species. These alterations would be based on microfluidic principles of chaotic mixing.

When working with typical microfluidic channels, it's important to note that one is normally working with a very low Reynold's (*Re*) number ($Re << 1$).[104,136] The Reynold's number is a ratio between the inertial forces and vicious forces acting on a small amount of fluid. In the case of low Reynold's numbers, laminar flow or streamline flow, is present.[137] This streamline flow is the type of flow observed in simple diffusion designs (**Figure 3.5A**). When the two fluids combine in the T-junction a limited diffusion zone, indicated by the green section in **Figure 3.5B**, is created.[138] Therefore much of the two fluids are left unmixed. Typical approaches to fix this issue include increasing the channel length until the limited diffusion zone extends to the full width of the channel and altering the flow speeds of reacting fluids[139], yet in the case of paper microfluidics these approaches are impractical due to limited solvent amounts and capillary flow restrictions.

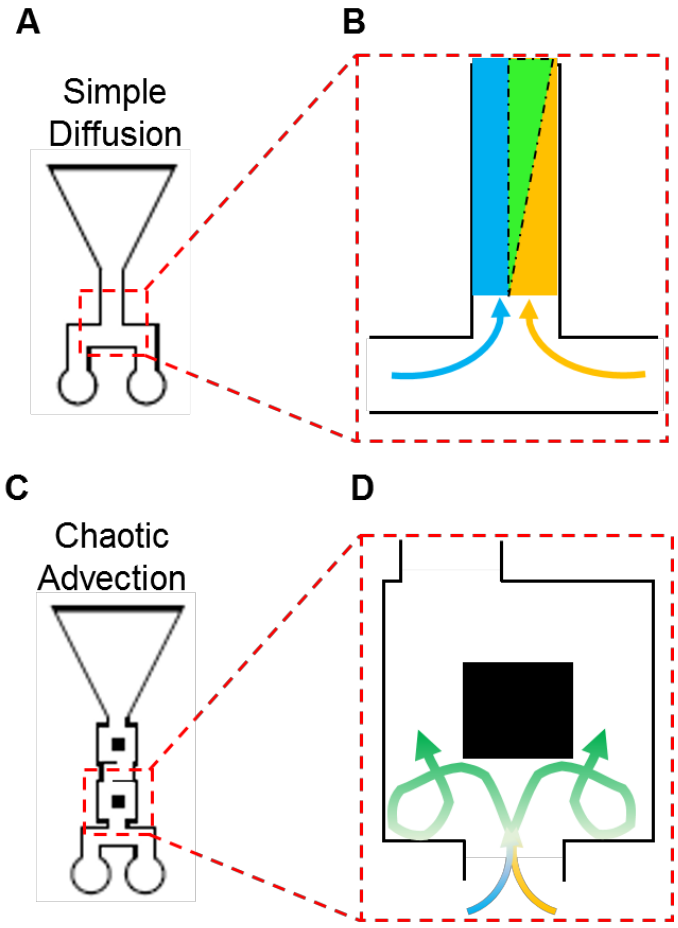

Figure 3.5: **(A)** Design for simple diffusion mixing. **(B)** Close-up image of T-junction where mixing occurs in the simple diffusion design. **(C)** Design for the chaotic mixing. **(D)** Close-up image of a first section where mixing occurs in the chaotic advection design.

Without turbulent flow, indicative of a high Reynold's number, mixing in microfluidic devices relays on diffusion alone, which is an inherently arduous and inefficient process.[118] Many passive microfluidic mixing regimes focus on improving efficiency by increasing the contact time by various methods.[122-124,140] Therefore we purpose utilizing a slightly modified passive mixing design, as seen in **Figure 3.5C** and **A.5H**, created by Nguyen and coworkers, which improves mixing by increasing chaotic advection, better known as chaotic mixing.[124] In

this design, there are a combination of channel width changes and physical obstacles. These obstructions create both small eddies, as seen in **Figure 3.5D**, and a slower flow rate. In conjunction these effects should increase the contact time between reacting species. This increase in contact time and physical mixing by the eddies, should yield a more complete reaction.

. While this design was initially successful on a quartz chip, significant analysis will be needed to determine its feasibility on paper. Unlike other microfluidic substrates, paper fibers are hydrophilic and absorbs small amounts of both the mobile solvent and the analyte, thereby decreasing the total concentration downstream. By creating channels which slow the solvent speed down to increase reaction time, there might be an adverse effect in material uptake due to the paper's fibrous structure. Also, extensive fabrication analysis will be needed to determine the ideal channel and obstructive size as to both not cut off a channel and make the design reproducible and scalable.

CHAPTER 4 COUPLING 3D PAPER MICROFLUIDICS TO PAPER SPARY MASS SPECTROMETRY

4.1 Introduction

Table 4.1: List of on-chip treatments that have been incorporated into µTAS.

Treatment Type	Treatment
Separation	Capillary Electrophoresis
Separation	RP HPLC
Derivatization	Alkylation
Desalting	Microdialysis
Desalting/Preconcentration	Solid Phase Extraction
Preconcentration	Sample Stacking
Preconcentration	Immunoaffinity
Electrochemistry	Voltammertry

Over the last couple decades miniaturized total chemical analysis systems (µTAS) have had several interesting and useful sample treatments, several of which can be seen in **Table 4.1**, integrated on-chip.[54] These treatments, or chip functionalizations, are particularly beneficial to µTAS coupled with electrospray ionization sources. As these coupled devices analyze increasingly complex samples such as protein mixtures[141], whole cell lysates[142], and metabolite monitoring[143], means of separating and concentrating analytes must be undertaken to ensure sensitive detection. Recently, several of these functionalizations have been created in series on their respective chips allowing for even greater cleanup before analysis. This incorporation of additional functionalizations is achieved by altering the hydrophobicity of the substrate or altering the channels dimensions, both of which are easily done with currently used µTAS substrates.[54]

While many of the functionalizations have been transferred to microfluidic paper-based analytical devices (μPADs), only one or two functionalizations can be incorporated at a time. This is due to inherent limitations of both the substrate and device. μPADs have an inherent size limitation as, unlike μTAS, the substrate absorbs both solvent and material.[144] Therefore increasing the size of a μPAD is impractical. This limitation is made more pertinent when sample volumes are limited, which is a common condition with μPADs. Also unlike μTAS, there are limitations on how much the lengths and widths of imprinted channels in μPADs can be altered. Therefore, new methodologies are required to increase the number of on-substrate treatments while simultaneously minimizing the total size of the substrate.

Initial work in the fields of μTAS and μPAD analysis revolved around 1 and 2-dimensional flow, or in the x,y plane of the substrate.[145] It wasn't until advances in fabrication techniques and 3D printing, that 3D μTAS were possible[146-148]. Tapping into the z-direction, or the depth of the device, is of particular interest as the length of the z-direction is shorter than in the x,y plane.[144] These 3D devices allowed for greater incorporation of treatments and the potential of multiplexing experiments on a single chip. While successful, these devices can required expensive facilities, instrumentation, and software. In 2008 Whitesides[149], demonstrated that stacking layers of paper and tape into a 3D μPAD could have similar capabilities as early 3D μTAS. These 3D μPADs have the additive advantage of being flexible and far easier to use and create than 3D μTAS. The creation of 3D μPADs opened a new door in creating simplistic diagnostic devices in a host of areas.

Much like their 2D predecessors, 3D µPADs relied on primarily on colorimetric, fluorometric, electrochemical signals.[57] These detection methods, although sensitive and specific for their particular analyses, pale in comparison to the achievable specificity of mass spectrometry.[53] Yet, there are some immediate questions that have to be answered before coupling between 3D µPADs and mass spectrometry can occur. 3D µPADs have shown adequate analyte detection after up to 8 paper connections when using fluorometric and colorimetric detection methods.[149] And while accessing the z-direction to add more functionalizations would be beneficial for sample treatment, adding to many layers could lead to detrimental sample loss. Therefore the number of paper layers, and by extension the number of possible functionalizations, in relation to detectable output needs to be analyzed.

Herein, we examine the potential for sample loss when using 3D µPADs and identify the maximum number of layers that can be used before detrimental signal loss occurs. While 3D µPADs have shown acceptable signal after 8 paper connections, these results have been with non-mass spectrometry detection methods. We also demonstrate the potential for coupling a simple 3D µPAD, with a cation exchange functionalization, to a paper spray device for pesticide detection – underlying the capabilities of these devices for real world applications.

4.2 Materials and Methods

Materials

Propazine, and rhodamine 6G dye (R6G) were obtained from Sigma-Aldrich (St. Louis, MO). High performance liquid chromatography (HPLC) grade methanol and water was from Burdick and Jackson (Muskegon, MI). Whatman grade 1 filter paper sheets of were purchased

from GE Healthcare Bio-Sciences (Pittsburgh, PA). Cation exchange paper was purchased from CTL Scientific Supply Corp (Deer Park, NY). All mass analyses were performed using a Q Exactive Plus Orbitrap mass spectrometer (Thermo Scientific, Bremen, Germany).

Sample Loss by Layer

Square pieces of paper with a single wax-printed well **(Figure A.5I)** were fabricated and stacked on a triangular piece of paper with wax-printed barriers **(Figure A.5E)**. Square pieces were either absent or stacked one, two, or three layers high. 10 µl of a 100 µM solution of propazine or R6G dye was pipetted in the middle of the top well, or middle of the wax-printed triangular piece if no layers were stacked on top. The layers were pressed together to allow for vertical transport and held for one minute. Final triangles were then cut, loaded with 50 µl of methanol/water (1:1, v/v), and tandem mass spectrometry (MS/MS) was performed on either the protonated propazine or R6G parent ion (*m/z* 230 and 445 respectively). The primary fragment ions (*m/z* 188 and 415 respectively) was isolated and used to compare each design's loss per layer. Results were recorded for one minute.

Soil Test – Cation Exchange

A small disk of cation exchange paper was punched out using a hand hole punch. The cation exchange disk was placed between a singular piece of both a wax-printed circular well **(Figure A.5I)** and a triangular piece of paper with wax-printed barriers **(Figure A.5E)**. A 10 ml sample of fresh soil was collected from outside the North Carolina State Toxicology building. A .5 ml eppendorf tube was filled with soil, approximately 4 grams, and spiked with 5µl of a 1 µM sample of propazine and stirred. The sample was allowed to dry in ambient air

for one hour. The complete contents of the eppendorf tube was loaded onto the paper well, the three layers pressed together, and washed with 50µl of a methanol/water solution (1:1, v/v). The bottom triangle with wax-printed barriers was then cut, loaded with 50 µl of methanol/water (1:1, v/v), and tandem mass spectrometry (MS/MS) was performed on the protonated propazine parent ion (*m/z* 230). The primary fragment ion (*m/z* 188) was isolated. A new triangle with wax-printed barriers was loaded underneath the cation exchange disc and the soil was removed from the top layer. 50µl of a 100µM solution of ammonium hydroxide was added to the top layer to elute the caught propazine. The bottom triangle with wax-printed barriers was then cut, loaded with 50 µl of methanol/water (1:1, v/v), and tandem mass spectrometry (MS/MS) was performed on the protonated propazine parent ion (*m/z* 230). The primary fragment ion (*m/z* 188) was isolated to compare wash against elution. Analysis when only using a physical top layer filter was also conducted for both compounds. All results were recorded for one minute.

4.3 Results and Discussion

4.3.1 Sample Loss by Layer

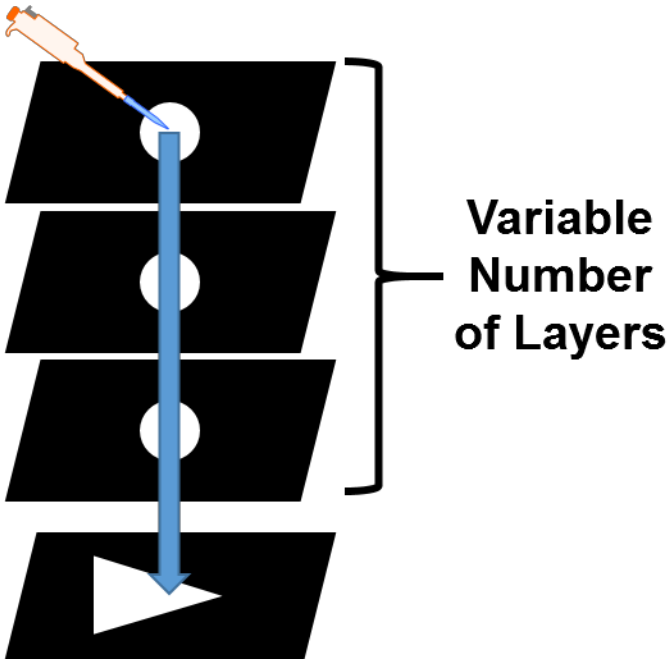

Figure 4.1: Schematic of the setup used in determined amount of sample lost per layer in 3D microfluidic devices. A maximum of three layers was used in determining sample loss.

Figure 4.1 shows the workflow for the determination of sample lost per paper layer in a simple wax-printed 3D microfluidic paper analytical device coupled to paper spray ionization, 3D-µPAD-PS. Although there are several materials and compounds used as connecting material between the paper layers including cellulose powder[149] and commercially available adhesive compounds[145], our analyses used direct contact between paper layers as to eliminate any non-paper material absorbing sample. This direct contact method is prevalent in several 3D paper devices, especially origami paper-based devices (*o*PADs) created by Richard Crooks.[150] It should be noted that although the layers were designed to directly sit on top of

each other and provide a straight vertical route for sample flow, layers occasionally “slid” off each other leading to failed runs. Also, if the sample wells were not equal in size then the sample fluid did occasionally “spill” out and sit between the wax-printed layers. In total these types of errors occurred in less than 5% of all runs Due to this potential for increased human error with each subsequent layer added, a maximum of 3 paper layers were used.

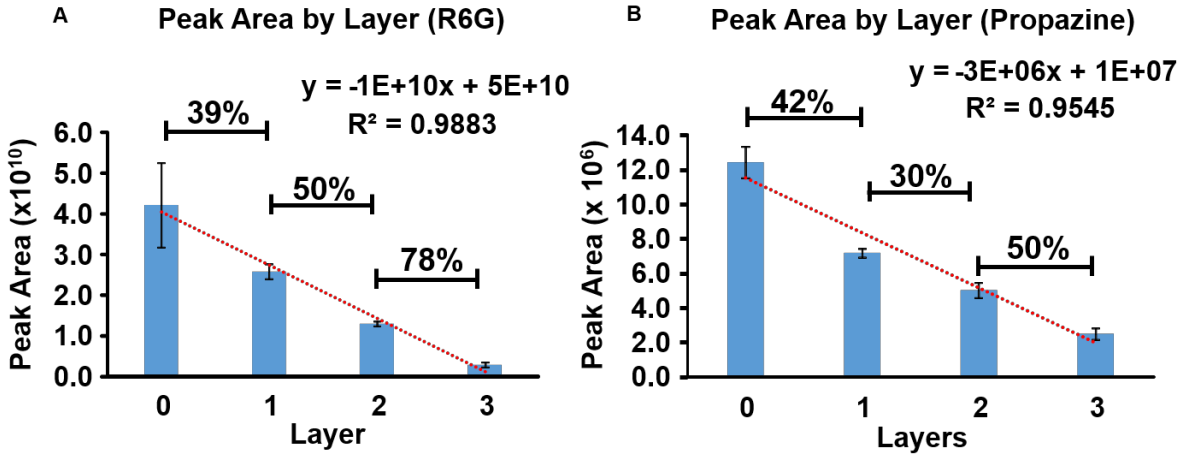

Figure 4.2: Average peak area by layer for **(A)** R6G and **(B)** Propazine. Linear regression and percentage of sample lost between adjacent layers is included for each compound.

To determine the amount of sample lost by layering paper, a 10 µl neat solution of either 100 µM propazine or R6G dye was loading and allowed to flow to the final zone by physical compression. This final zone, layer “0” in **Figure 4.2**, was cut and analyzed in triplicate. The average peak area at each layer can been seen in **Figure 4.2**, linear regression was also performed to determine the rate of sample loss. With both compounds, there was a highly correlated ($R^2 < 0.95$) decrease in total peak area with the addition of subsequent layer. Loss between sequential layers ranged from 30-78% and between direct analysis (0 layers) and 3 layers, roughly an order-of-magnitude in peak area was lost. This loss is significant to note, as samples most likely to be tested by a 3D-µPAD-PS device, similar to other paper spray

analyses, will be in much lower concentrations (<<10μM) and an order-of-magnitude loss could prove to be significant. Interestingly, the use of paper layers decreased the variance of each layer set in comparison to direct analysis. Variance between direct analysis and each layer was compared via f-test with an alpha value of 0.05; only the variance changes in R6G were found to be significant ($p < 0.05$).

Significant research has gone into increasing the transport capabilities in the z-direction such as changing the paper permeability[151] and directly connecting adjacent layers[145,149,152,153]. Yet, these techniques require additional fabrication resources and the potential addition of compounds that could increase signal background or react with the target analyte. Therefore, the potential addition of two vertical layers was deemed an acceptable "cost" for the potential benefit of incorporating useful functionalizations in the z-direction. It is important to note that these results are only for Whatman Grade 1 filter paper, with a depth of ~180 μm, and different brands of paper would need to be tested individually.

4.3.2 Soil Test - Cation Exchange

To test the capability of using z-directional functionalization to increase paper spray's versatility, we examined the use of cation exchange paper to concentrate the pesticide propazine in a collected soil sample. Commercially sold soils, such as Miracle-Gro®, contains dozens of organic compounds and minerals[154], and industrial agricultural soil contains hundreds of additives on top of the organic matter and minerals.[155] A poplar class of additives include the triazine herbicides, of which the three most commonly used are atrazine, propazine, and simazine. Their structures and industrial usage rates by can been seen in **Figure 4.3**.

Although popular due to their effectiveness, these compounds are also noted as having drastic human health consequences. In particular, atrazine is a known endocrine disruptor amongst other things.[156] Therefore, monitoring and detection of these potentially harmful compounds is a pressing concern for public health.

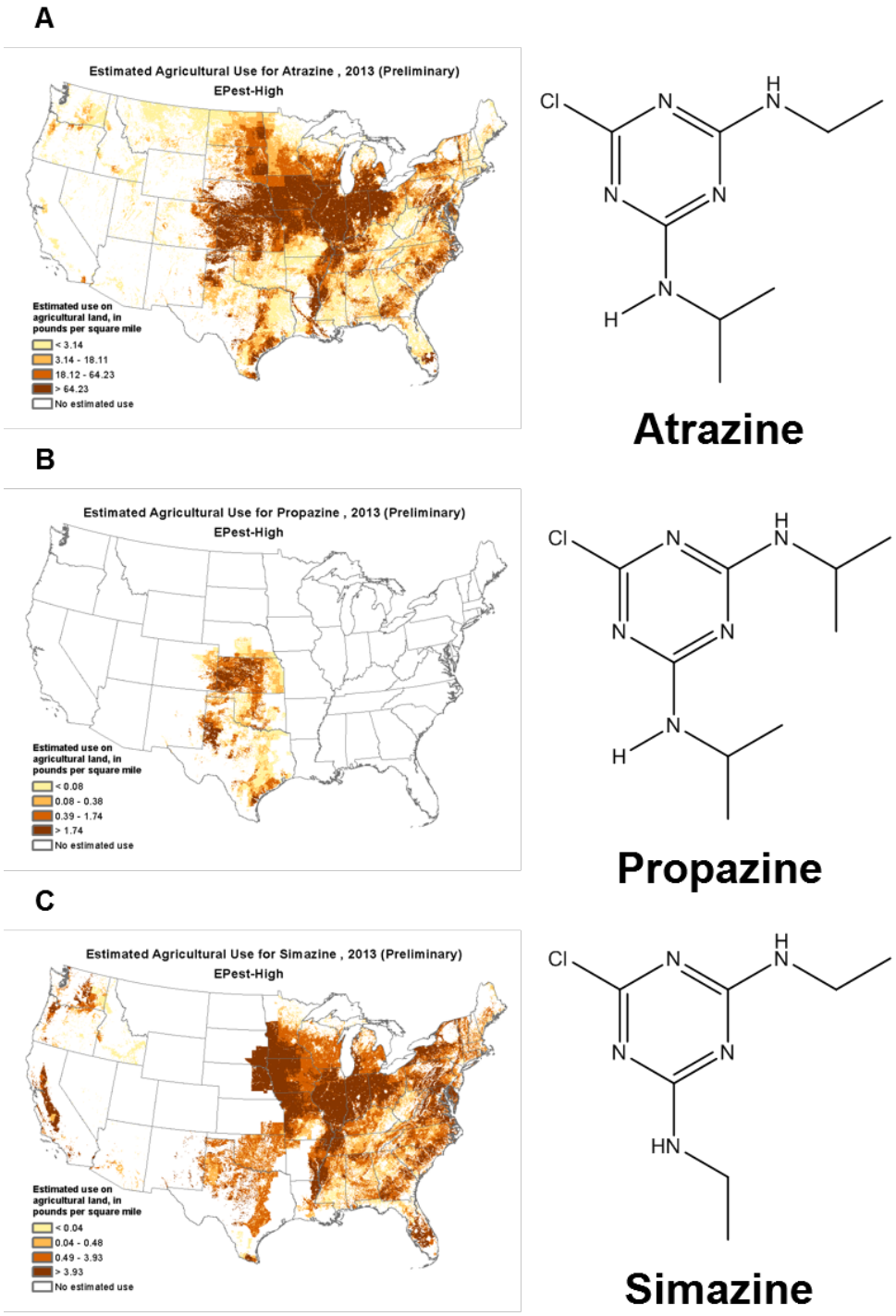

Figure 4.3: United State Environmental Protection Agency's estimated agricultural use for **(A)** atrazine **(B)** propazine and **(C)** simazine. Their structures are also included.[2]

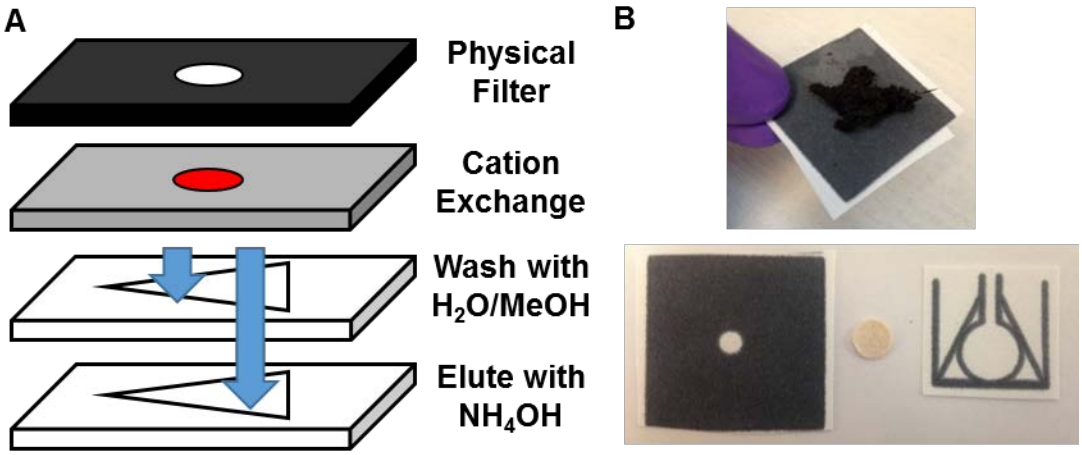

Figure 4.4: **(A)** Schematic of cation exchange 3D-paper device. **(B)** Images of a loaded soil sample and the 3D device.

A schematic and images for testing can be seen in **Figure 4.4A** and **B** respectively. As stated in the aforementioned section, a maximum of two additional layers were used in order to minimize layer loss. It should also be noted that the second layer, the cation exchange disc, is significantly thicker than the Whatman Grade 1 filter paper and presumably has a decreased porosity due to the derivatized cellulose fibers. The top layer acted as a solid filter allowing for both soluble compounds, including the spiked in propazine, to freely move to the second layer and the removal of large particulate. The second layer consisted of a punched-out disc of cation exchange paper. As mentioned the previous section this physical stacking proved be laborious and prone to the occasional slipping error. A solution of 100 µM ammonium hydroxide was used to competitively elute the bound pesticide. A common concern with paper-based technologies is their stability, under different solvent systems.[49] Therefore, it should be

noted that the addition of 100 µM ammonium hydroxide showed no adverse effects to either the paper or the wax-printed barriers.

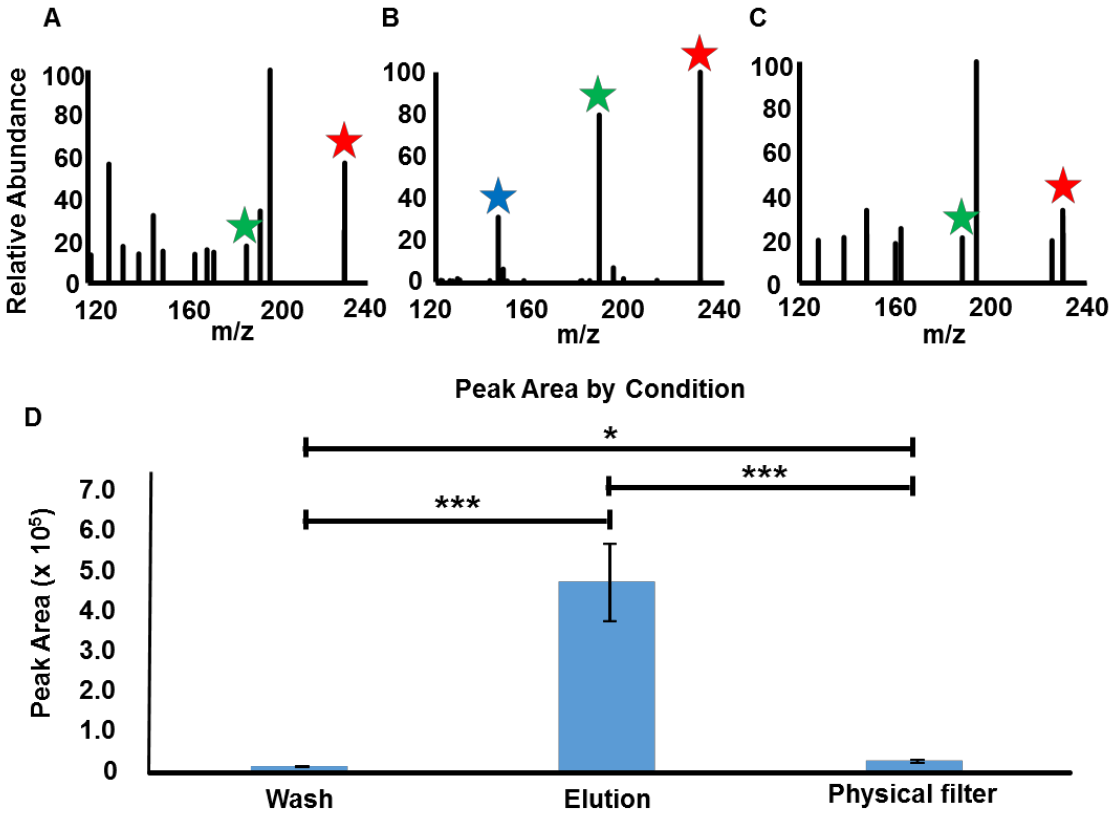

Figure 4.5: Representative spectra for **(A)** Water:MeOH wash **(B)** Elution wash and **(C)** Water:MeOH wash using only a physical filter. Stars represent propazine ions: (red, *m/z* 230), (green, *m/z* 188), and (blue, *m/z* 146). **(D)** Peak area comparisons under each conditions. Standard error bars are include for each condition. Stars (*) represent the degree of significance in difference between conditions: (*, $p < 0.05$) and (***, $p < 0.01$).

Spectra and peak analysis was performed both the wash and elution collections. Representative spectra can be seen in **Figure 4.5A** and **B**, respectively. While in theory the wash collection should not contain detectable amounts of the pesticide, as it should have been collected in the cation exchange disc, it is possible due that saturation of the disc led to fluid moving “around” the disc and being absorbed into the collection layer. A third set of analyses was performed by washing the soil through the physical filter without an intermediate cation

exchange disc. This was done to assess the effectiveness of solely using a physical filter in removing the soil matrix and ion suppressant compounds. A representative spectra can be seen in **Figure 4.5C**. An interesting observation is the absence of the second transition ion (*m/z* 146, blue star) of propazine in either the wash or physical filter spectra. This ion is formed by the loss of both propylene groups on propazine.[127] This lack of the second transition ion is most likely due to either a low collection on the propazine pesticide or significant suppression in both of these conditions. This suppression is probability from salt and phosphate additives, which would pass though both the cation exchange disc and physical filter, commonly found in commercial soil.[157] This ability to use a functionalized intermediate layer to effectively filter out unwanted compounds is also evident by the "cleanliness" of the elution spectra in relation to the other two.

Peak areas of the primary transition ion (*m/z* 188) were collected under each condition and in triplicate to compare detection capabilities, as seen in **Figure 4.5D**. While there was a relatively minor, yet significant ($p < 0.05$) as determined by a Welsh's t-test, difference in the peak area between the wash and physical filter conditions both condition's average peak area was over two orders-of-magnitude less than the elution's. The difference in peak areas between the elution condition and both the wash and physical filter were very significant ($p < 0.01$). It's interesting to note that average peak area under the elution condition was an order-of-magnitude less than the average peak area while using two layers of paper, as seen in **Figure 4.2B**. Although these conditions were considered equivalent, both the extra thickness of the cation exchange discs and limited extraction of the spiked in propazine likely account for this

discrepancy. These results indicate the potential of using functionalized intermediate layers as means to increase paper sprays versatility, instead of incorporating equivalent functionalizes in the plane of the paper itself. These results also demonstrate the potential for a simplistic paper spray device to be used as a monitoring tool for a public health hazard.

4.4 Conclusions

Paper spray mass spectrometry (PS) is a simple analytical technique yet, for it to expand its versatility and application usage, more advanced microfluidic paper analytical device (µPAD) on-substrate treatments must be incorporated. Due to size and sample limitations inherent with µPAD techniques[144], and therefore potential µPAD-PS devices, several avenues must be pursued in order to maximize functionality within a confined amount of space. In 2D µPAD devices the predominate manner of incorporating possible treatments is by altering the channel's lengths and widths[144,158], but there are limitations to this method. And while other avenues of research such as altering the paper's porosity and permeability has begun to take place, work is limited. Recently, work into creating 3D µPADs has been undertaken as a means to overcome several of the limitations with 2D µPAD. By utilizing the z-direction (depth) a 3D µPAD can both use a shorter free path and perform multiplexed manipulations. Herein, the feasibility of using 3D µPADs coupled to PS is explored and a prototype of a real world 3D-µPAD-PS is demonstrated.

Wax-printed layers, utilizing the z-direction as the primary fluid path, led to a linear decrease in total detected peak area with the addition of each additional layer for two compounds. After the addition of three layers roughly an order-of-magnitude in peak area was

lost. This loss could prove to be detrimental in later analyses, therefore a maximum of two layers was determined to be acceptable in later experiments. A reduction in variability was also noticed in comparison between direct analysis (0 layers) and each subsequent layer. This reduction was only determined to be significant ($p < 0.05$) by f-test for one compound.

A simple 3D-µPAD-PS was fabricated, consisting of a physical paper filter and a cation exchange disc on top a final paper spray receptacle, to examine the feasibility of using functionalized layers a 3D-µPAD-PS. Fresh soil spiked with the pesticide propazine was washed with a Water:MeOH solution and the bound propazine was eluted with a relatively concentrated ammonium hydroxide solution. A third analysis using only the physical layer was performed to assess the cation exchange disc's performance. A significant difference ($p <.01$) in peak area, of roughly 2 orders-of-magnitude, was observed between the elution and both the wash and physical filter conditions. Also, an easily discernable "cleanliness" was observed in the elution spectra in comparison to both the wash and physical filter spectra. These results make evident the potential of using 3D functionalization as a means to increase the versatility of a simple paper spray device. Future experiments will explore the potential of creating a duplex device with both real-time and mass spectrometric confirmatory detection methods.

4.5 Ongoing and Future Work

4.5.1 Field Deployable Devices

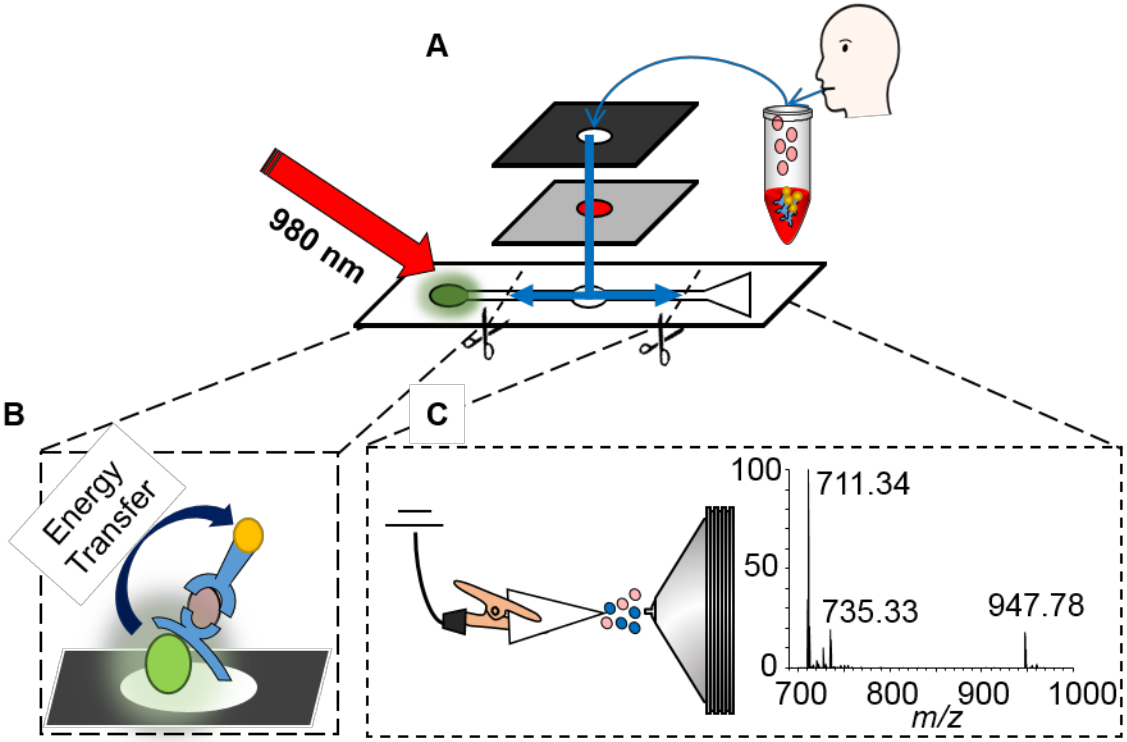

Figure 4.6: **(A)** Development of an integrated system for the dual detection of targeted analytes in a 3D paper spray microfluidic device. **(B)** Proposed aptamer-based fluorescent detection method. **(C)** Confirmatory paper spray analysis.

With an ever increasing global population, expansion in global agricultural output will be a necessity.[159] This demand for agricultural products will lead many developing countries to adopt effective, yet simultaneously harmful, pesticide usage habits to increase output. As seen in America and several other developed countries, pesticide usage can have disastrous effects on public health.[160] To ensure a healthy global population in resource stricken areas, cost-effective monitoring and diagnosis techniques must be implemented. This demand is where µTAS and µPAD assays excel.

A majority of μTAS and μPAD assays use colorimetry, electrochemistry, electrochemiluminescence, and chemiluminescence as the primary detection techniques.[50] While these detection techniques are particularly well suited for immediate on-site detection, due to their typical binary response of "yes" or "no" signals[57,64,74,104,105], quality clinical detection devices need to have highly sensitivity confirmatory tests that can be used to validate initial responses and reduce the occurrence of false positives. Therefore, we propose the creation of a 3D μPAD with dual detection capabilities. After some type of sample treatment to remove unwanted particulate, including but not limited to the use of a physical filter and cation exchange as detailed in the aforementioned work, the sample would be split between a receptacle for immediate detection and a paper spray triangle for later laboratory confirmation.

In particular, we propose using an aptamer based fluorescent detection method. Aptamers are relatively short oligonucleotides that have been designed for specific binding to particular compounds, usually by using a process called Systematic Evolution of Ligands by Exponential Enrichment (SELEX).[161,162] By using SELEX, aptamers can be customized for almost any particular public health demand. These aptamers can be bound to various fluorescent molecules such as gold nanoparticles[163], upconversion crystals[164-166], and quantum dots[167,168], all of which can create both a visible identification and a ranged response that is dependent on the analytes concentration. Dependent on the response from the initial fluorometric detection, confirmatory analysis via paper spray can be performed. It should also be mentioned that paper spray is an excellent candidate for off-site confirmatory tests as paper is noted as maintaining compound stability in the substrates matrix, even in harsh conditions.[169]

These type of devices could have a both a global impacts as well as a local ones, as monitoring for compounds released from the Duke Energy coal ash spill has become a major research goal for North Carolina's Department of Environmental Quality and topic in the State's Legislature.

REFERENCES

(1) University, N. D. S.

(2) United State Geological Survey Online, 2013.

(3) Nobel Media: Nobelprize.org.

(4) Fenn, J. B. *Journal of the American Society for Mass Spectrometry* **1993**, *4*, 524-535.

(5) Karas, M.; Bachmann, D.; Hillenkamp, F. *Analytical Chemistry* **1985**, *57*, 2935-2939.

(6) Tanaka, K.; Waki, H.; Ido, Y.; Akita, S.; Yoshida, Y.; Yoshida, T.; Matsuo, T. *Rapid communications in mass spectrometry* **1988**, *2*, 151-153.

(7) Soltwisch, J.; Jaskolla, T. W.; Hillenkamp, F.; Karas, M.; Dreisewerd, K. *Analytical chemistry* **2012**, *84*, 6567-6576.

(8) Jaskolla, T. W.; Karas, M. *Journal of the American Society for Mass Spectrometry* **2011**, *22*, 976-988.

(9) Lu, I.-C.; Lee, C.; Lee, Y.-T.; Ni, C.-K. *Annual Review of Analytical Chemistry* **2015**, *8*, 21-39.

(10) Alberici, R.; Simas, R.; Sanvido, G.; Romão, W.; Lalli, P.; Benassi, M.; Cunha, I. S.; Eberlin, M. *Analytical and Bioanalytical Chemistry* **2010**, *398*, 265-294.

(11) Takats, Z.; Wiseman, J. M.; Gologan, B.; Cooks, R. G. *Science* **2004**, *306*, 471-473.

(12) Cody, R. B.; Laramée, J. A.; Durst, H. D. *Analytical Chemistry* **2005**, *77*, 2297-2302.

(13) McEwen, C. N.; McKay, R. G.; Larsen, B. S. *Analytical Chemistry* **2005**, *77*, 7826-7831.

(14) Sampson, J. S.; Hawkridge, A. M.; Muddiman, D. C. *Journal of the American Society for Mass Spectrometry* **2006**, *17*, 1712-1716.

(15) Lebedev, A. b. T. *Russian Chemical Reviews* **2015**, *84*, 665.

(16) Ouyang, Z.; Cooks, R. G. *Annual Review of Analytical Chemistry* **2009**, *2*, 187-214.

(17) Chen, H.; Gamez, G.; Zenobi, R. *Journal of the American Society for Mass Spectrometry* **2009**, *20*, 1947-1963.

(18) Davy, J. *Philosophical Transactions of the Royal Society of London* **1812**, *102*, 144-151.

(19) Ettre, L. S. *LC GC North America* **2001**, *19*, 506-512.

(20) Consden, R.; Gordon, A. H.; Martin, A. *Biochemical Journal* **1944**, *38*, 224.

(21) Liu, J.; Wang, H.; Manicke, N. E.; Lin, J.-M.; Cooks, R. G.; Ouyang, Z. *Analytical chemistry* **2010**, *82*, 2463-2471.

(22) Snyder, D. T.; Pulliam, C. J.; Ouyang, Z.; Cooks, R. G. *Anal Chem* **2015**.

(23) Espy, R. D.; Muliadi, A. R.; Ouyang, Z.; Cooks, R. G. *International Journal of Mass Spectrometry* **2012**, *325*, 167-171.

(24) Espy, R. D. *Fundamentals, method development, and applications of paper spray ionization mass spectrometry*. PURDUE UNIVERSITY2014.

(25) Shi, R.-Z.; El Gierari, E.; Faix, J. D.; Manicke, N. E. *Clinical chemistry* **2015**.

(26) Shi, R.-Z.; El Taher, M.; Manicke, N. E.; Faix, J. D. *Clinica Chimica Acta* **2015**, *441*, 99-104.

(27) Espy, R. D.; Teunissen, S. F.; Manicke, N. E.; Ren, Y.; Ouyang, Z.; van Asten, A.; Cooks, R. G. *Analytical chemistry* **2014**, *86*, 7712-7718.

(28) Yang, Q.; Manicke, N.; Wang, H.; Petucci, C.; Cooks, R. G.; Ouyang, Z. *Analytical and Bioanalytical Chemistry* **2012**, *404*, 1389-1397.

(29) Zhang, Z.; Xu, W.; Manicke, N. E.; Cooks, R. G.; Ouyang, Z. *Analytical Chemistry* **2012**, *84*, 931-938.

(30) Manicke, N. E.; Yang, Q.; Wang, H.; Oradu, S.; Ouyang, Z.; Cooks, R. G. *International Journal of Mass Spectrometry* **2011**, *300*, 123-129.

(31) Manicke, N. E.; Bills, B. J.; Zhang, C. *Bioanalysis* **2016**, *8*, 589-606.

(32) Wang, H.; Ren, Y.; McLuckey, M. N.; Manicke, N. E.; Park, J.; Zheng, L.; Shi, R.; Cooks, R. G.; Ouyang, Z. *Analytical Chemistry* **2013**, *85*, 11540-11544.

(33) Wang, H. **2012**.

(34) Prosolia.

(35) Vega, C.; Spence, C.; Zhang, C.; Bills, B. J.; Manicke, N. E. *Journal of The American Society for Mass Spectrometry* **2016**, 1-9.

(36) Espy, R. D.; Manicke, N. E.; Ouyang, Z.; Cooks, R. G. *Analyst* **2012**, *137*, 2344-2349.

(37) Zhang, Z.; Cooks, R. G.; Ouyang, Z. *Analyst* **2012**, *137*, 2556-2558.

(38) Han, F.; Yang, Y.; Ouyang, J.; Na, N. *Analyst* **2015**, *140*, 710-715.

(39) Zhang, C.; Manicke, N. E. *Analytical Chemistry* **2015**, *87*, 6212-6219.

(40) Salentijn, G. I.; Permentier, H. P.; Verpoorte, E. *Analytical chemistry* **2014**, *86*, 11657-11665.

(41) Johnson, R. W. *Handbook of fluid dynamics*; Crc Press, 1998.

(42) Whitesides, G. M. *Nature* **2006**, *442*, 368-373.

(43) Manz, A.; Harrison, D. J.; Verpoorte, E. M.; Fettinger, J. C.; Paulus, A.; Lüdi, H.; Widmer, H. M. *J. Chromatogr. A* **1992**, *593*, 253-258.

(44) Nikolelis, D. P.; Varzakas, T.; Erdem, A.; Nikoleli, G.-P. *Portable Biosensing of Food Toxicants and Environmental Pollutants*; CRC Press, 2013.

(45) Manz, A.; Miyahara, Y.; Miura, J.; Watanabe, Y.; Miyagi, H.; Sato, K. *Sensors and Actuators B: Chemical* **1990**, *1*, 249-255.

(46) Manz, A.; Graber, N.; Widmer, H. M. *Sensors and Actuators B: Chemical* **1990**, *1*, 244-248.

(47) Reyes, D. R.; Iossifidis, D.; Auroux, P.-A.; Manz, A. *Analytical Chemistry* **2002**, *74*, 2623-2636.

(48) Martinez, A. W.; Phillips, S. T.; Butte, M. J.; Whitesides, G. M. *Angewandte Chemie (International ed. in English)* **2007**, *46*, 1318-1320.

(49) Yetisen, A. K.; Akram, M. S.; Lowe, C. R. *Lab on a Chip* **2013**, *13*, 2210-2251.

(50) Xu, Y.; Liu, M.; Kong, N.; Liu, J. *Microchimica Acta* **2016**, 1-22.

(51) Lin, Y.; Gritsenko, D.; Feng, S.; Teh, Y. C.; Lu, X.; Xu, J. *Biosensors and Bioelectronics* **2016**.

(52) Liu, H.; Xiang, Y.; Lu, Y.; Crooks, R. M. *Angewandte Chemie* **2012**, *124*, 7031-7034.

(53) Wang, X.; Yi, L.; Mukhitov, N.; Schrell, A. M.; Dhumpa, R.; Roper, M. G. *J. Chromatogr. A* **2015**, *1382*, 98-116.

(54) Koster, S.; Verpoorte, E. *Lab on a Chip* **2007**, *7*, 1394-1412.

(55) Why Population Matters to Infectious Diseases and HIV/AIDS; Population Action International 2011.

(56) Patabadige, D. E.; Jia, S.; Sibbitts, J.; Sadeghi, J.; Sellens, K.; Culbertson, C. T. *Analytical chemistry* **2015**, *88*, 320-338.

(57) Lisowski, P.; Zarzycki, P. *Chromatographia* **2013**, *76*, 1201-1214.

(58) Kovarik, M. L.; Ornoff, D. M.; Melvin, A. T.; Dobes, N. C.; Wang, Y.; Dickinson, A. J.; Gach, P. C.; Shah, P. K.; Allbritton, N. L. *Analytical Chemistry* **2013**, *85*, 451-472.

(59) Yagoda, H. *Industrial & Engineering Chemistry Analytical Edition* **1937**, *9*, 79-82.

(60) Müller, R. H.; Clegg, D. L. *Analytical Chemistry* **1949**, *21*, 1123-1125.

(61) Clarke, S.; Foster, J. *British journal of biomedical science* **2012**, *69*, 83.

(62) NIH.

(63) Chard, T. *Human reproduction* **1992**, *7*, 701-710.

(64) Mark, D.; Haeberle, S.; Roth, G.; von Stetten, F.; Zengerle, R. *Chemical Society Reviews* **2010**, *39*, 1153-1182.

(65) Verpoorte, E. *Electrophoresis* **2002**, *23*, 677-712.

(66) Marle, L.; Greenway, G. M. *TrAC Trends in Analytical Chemistry* **2005**, *24*, 795-802.

(67) Yamashita, M.; Fenn, J. B. *The Journal of Physical Chemistry* **1984**, *88*, 4451-4459.

(68) Wilm, M.; Mann, M. *Analytical chemistry* **1996**, *68*, 1-8.

(69) Wang, H.; Manicke, N. E.; Yang, Q.; Zheng, L.; Shi, R.; Cooks, R. G.; Ouyang, Z. *Analytical chemistry* **2011**, *83*, 1197-1201.

(70) Su, Y.; Wang, H.; Liu, J.; Wei, P.; Cooks, R. G.; Ouyang, Z. *Analyst* **2013**, *138*, 4443-4447.

(71) Cate, D. M.; Adkins, J. A.; Mettakoonpitak, J.; Henry, C. S. *Analytical chemistry* **2014**, *87*, 19-41.

(72) Chen, B.; Kwong, P.; Gupta, M. *ACS applied materials & interfaces* **2013**, *5*, 12701-12707.

(73) Carvalho, T. C.; Garcia, P. T.; Campanha, R. B.; Abdelnur, P. V.; Romão, W.; Coltro, W. K. T.; Vaz, B. G. *Analyst* **2016**.

(74) Li, X.; Ballerini, D. R.; Shen, W. *Biomicrofluidics* **2012**, *6*, 011301.

(75) Li, X.; Tian, J.; Shen, W. *Cellulose* **2010**, *17*, 649-659.

(76) Martinez, A. W.; Phillips, S. T.; Whitesides, G. M.; Carrilho, E. *Analytical chemistry* **2009**, *82*, 3-10.

(77) del Campo, A.; Greiner, C. *Journal of Micromechanics and Microengineering* **2007**, *17*, R81.

(78) Lu, Y.; Shi, W.; Jiang, L.; Qin, J.; Lin, B. *Electrophoresis* **2009**, *30*, 1497-1500.

(79) Martinez, A. W.; Phillips, S. T.; Wiley, B. J.; Gupta, M.; Whitesides, G. M. *Lab on a Chip* **2008**, *8*, 2146-2150.

(80) Martinez, A. W.; Phillips, S. T.; Butte, M. J.; Whitesides, G. M. *Angewandte Chemie International Edition* **2007**, *46*, 1318-1320.

(81) Carrilho, E.; Martinez, A. W.; Whitesides, G. M. *Analytical chemistry* **2009**, *81*, 7091-7095.

(82) Huikko, K.; Ostman, P.; Grigoras, K.; Tuomikoski, S.; Tiainen, V. M.; Soininen, A.; Puolanne, K.; Manz, A.; Franssila, S.; Kostiainen, R.; Kotiaho, T. *Lab on a Chip* **2003**, *3*, 67-72.

(83) Chan, J. H.; Timperman, A. T.; Qin, D.; Aebersold, R. *Analytical Chemistry* **1999**, *71*, 4437-4444.

(84) Blanco, F.; Agirregabiria, M.; Berganzo, J.; Mayora, K.; Elizalde, J.; Calle, A.; Domínguez, C.; Lechuga, L. M. *Journal of Micromechanics and Microengineering* **2006**, *16*, 1006.

(85) Keller, B. O.; Sui, J.; Young, A. B.; Whittal, R. M. *Analytica chimica acta* **2008**, *627*, 71-81.

(86) Dentinger, P. M.; Clift, W. M.; Goods, S. H. *Microelectronic Engineering* **2002**, *61*, 993-1000.

(87) He, Y.; Wu, Y.; Xiao, X.; Fu, J.; Xue, G. *RSC Adv.* **2014**, *4*, 63860-63865.

(88) Yang, Q.; Wang, H.; Maas, J. D.; Chappell, W. J.; Manicke, N. E.; Cooks, R. G.; Ouyang, Z. *International journal of mass spectrometry* **2012**, *312*, 201-207.

(89) Nemes, P.; Marginean, I.; Vertes, A. *Analytical chemistry* **2007**, *79*, 3105-3116.

(90) Shen, L.; Zhang, J.; Yang, Q.; Manicke, N. E.; Ouyang, Z. *Clinica Chimica Acta* **2013**, *420*, 28-33.

(91) Wang, H.; Liu, J.; Cooks, R. G.; Ouyang, Z. *Angewandte Chemie* **2010**, *122*, 889-892.

(92) Manicke, N. E.; Abu-Rabie, P.; Spooner, N.; Ouyang, Z.; Cooks, R. G. *Journal of the American Society for Mass Spectrometry* **2011**, *22*, 1501-1507.

(93) Mazzotti, F.; Di Donna, L.; Taverna, D.; Nardi, M.; Aiello, D.; Napoli, A.; Sindona, G. *International Journal of Mass Spectrometry* **2013**, *352*, 87-91.

(94) Yan, X.; Augusti, R.; Li, X.; Cooks, R. G. *ChemPlusChem* **2013**, *78*, 1142-1148.

(95) Zhou, X.; Pei, J.; Huang, G. *Rapid Communications in Mass Spectrometry* **2015**, *29*, 100-106.

(96) Bain, R. M.; Pulliam, C. J.; Raab, S. A.; Cooks, R. G. *Journal of Chemical Education* **2016**, *93*, 340-344.

(97) Evard, H.; Kruve, A.; Lõhmus, R.; Leito, I. *Journal of Food Composition and Analysis* **2015**, *41*, 221-225.

(98) Duarte, L. C.; de Carvalho, T. C.; Lobo-Júnior, E. O.; Abdelnur, P. V.; Vaz, B. G.; Coltro, W. K. *Analytical Methods* **2016**, *8*, 496-503.

(99) Zhang, Y.; Li, H.; Ma, Y.; Lin, J.-M. *Analyst* **2014**, *139*, 1023-1029.

(100) Liu, W.; Chen, Q.; Lin, X.; Lin, J.-M. *Analyst* **2015**, *140*, 1551-1554.

(101) Campbell, T.; Williams, C.; Ivanova, O.; Garrett, B. *Technologies, Potential, and Implications of Additive Manufacturing, Atlantic Council, Washington, DC* **2011**.

(102) Narayanan, R.; Sarkar, D.; Cooks, R. G.; Pradeep, T. *Angewandte Chemie International Edition* **2014**, *53*, 5936-5940.

(103) Hilton, G. M.; Taylor, A. J.; McClure, C. D.; Parsons, G. N.; Bonner, J. C.; Bereman, M. S. *Toxicology* **2015**, *329*, 80-87.

(104) Stone, H. A.; Kim, S. *AIChE Journal* **2001**, *47*, 1250-1254.

(105) Dietzel, A. In *Microsystems for Pharmatechnology: Manipulation of Fluids, Particles, Droplets, and Cells*, Dietzel, A., Ed.; Springer International Publishing: Cham, 2016, pp 1-21.

(106) Medina, A.; Pérez-Rosales, C.; Pineda, A.; Higuera, F. *Revista mexicana de física* **2001**, *47*, 537-541.

(107) Colletes, T. C.; Garcia, P. T.; Campanha, R. B.; Abdelnur, P. V.; Romao, W.; Coltro, W. K. T.; Vaz, B. G. *Analyst* **2016**, *141*, 1707-1713.

(108) Lin, C.-H.; Liao, W.-C.; Chen, H.-K.; Kuo, T.-Y. *Bioanalysis* **2014**, *6*, 199-208.

(109) Enke, C. G. *Analytical Chemistry* **1997**, *69*, 4885-4893.

(110) Schmidt, A.; Karas, M.; Dülcks, T. *Journal of the American Society for Mass Spectrometry* **2003**, *14*, 492-500.

(111) Luo, Q.; Tang, K.; Yang, F.; Elias, A.; Shen, Y.; Moore, R. J.; Zhao, R.; Hixson, K. K.; Rossie, S. S.; Smith, R. D. *Journal of proteome research* **2006**, *5*, 1091-1097.

(112) Bereman, M. S.; Comins, D. L.; Muddiman, D. C. *Chemical Communications* **2010**, *46*, 237-239.

(113) Williams, D. K.; Comins, D. L.; Whitten, J. L.; Muddiman, D. C. *Journal of the American Society for Mass Spectrometry* **2009**, *20*, 2006-20012.

(114) Williams, D. K.; Meadows, C. W.; Bori, I. D.; Hawkridge, A. M.; Comins, D. L.; Muddiman, D. C. *Journal of the American Chemical Society* **2008**, *130*, 2122-2123.

(115) Bag, S.; Hendricks, P.; Reynolds, J. C.; Cooks, R. *Analytica chimica acta* **2015**, *860*, 37-42.

(116) Zhang, Y.; Ju, Y.; Huang, C.; Wysocki, V. H. *Analytical Chemistry* **2014**, *86*, 1342-1346.

(117) Hamid, A. M.; Jarmusch, A. K.; Pirro, V.; Pincus, D. H.; Clay, B. G.; Gervasi, G.; Cooks, R. G. *Analytical chemistry* **2014**, *86*, 7500-7507.

(118) Lee, C.-Y.; Chang, C.-L.; Wang, Y.-N.; Fu, L.-M. *International journal of molecular sciences* **2011**, *12*, 3263-3287.

(119) Rezk, A. R.; Qi, A.; Friend, J. R.; Li, W. H.; Yeo, L. Y. *Lab on a Chip* **2012**, *12*, 773-779.

(120) Fair, R. B. *Microfluidics and Nanofluidics* **2007**, *3*, 245-281.

(121) Fobel, R.; Kirby, A. E.; Ng, A. H.; Farnood, R. R.; Wheeler, A. R. *Advanced materials* **2014**, *26*, 2838-2843.

(122) Yang, J.-T.; Huang, K.-J.; Lin, Y.-C. *Lab on a Chip* **2005**, *5*, 1140-1147.

(123) Liu, R. H.; Stremler, M. A.; Sharp, K. V.; Olsen, M. G.; Santiago, J. G.; Adrian, R. J.; Aref, H.; Beebe, D. J. *Microelectromechanical Systems, Journal of* **2000**, *9*, 190-197.

(124) Nguyen, T.; Kim, M.-C.; Park, J.-S.; Lee, N.-E. *Sensors and Actuators B: Chemical* **2008**, *132*, 172-181.

(125) Wilm, M. S.; Mann, M. *International Journal of Mass Spectrometry and Ion Processes* **1994**, *136*, 167-180.

(126) Juraschek, R.; Dülcks, T.; Karas, M. *Journal of the American Society for Mass Spectrometry* **1999**, *10*, 300-308.

(127) Reeber, S. L.; Gadi, S.; Huang, S.-B.; Glish, G. L. *Analytical Methods* **2015**, *7*, 9808-9816.

(128) Soparawalla, S.; Tadjimukhamedov, F. K.; Wiley, J. S.; Ouyang, Z.; Cooks, R. G. *Analyst* **2011**, *136*, 4392-4396.

(129) Curwin, B. D.; Hein, M. J.; Sanderson, W. T.; Barr, D. B.; Heederik, D.; Reynolds, S. J.; Ward, E. M.; Alavanja, M. C. *J Expo Anal Environ Epidemiol* **2005**, *15*, 500-508.

(130) Bakke, B.; De Roos, A. J.; Barr, D. B.; Stewart, P. A.; Blair, A.; Freeman, L. B.; Lynch, C. F.; Allen, R. H.; Alavanja, M. C.; Vermeulen, R. *Journal of exposure science and environmental epidemiology* **2009**, *19*, 544-554.

(131) Malaj, N.; Ouyang, Z.; Sindona, G.; Cooks, R. G. *Analytical Methods* **2012**, *4*, 1913-1919.

(132) C.F.R, Ed., 2012.

(133) Agency, U. S. E. P., Ed., 2003.

(134) Fu, E.; Ramsey, S. A.; Kauffman, P.; Lutz, B.; Yager, P. *Microfluidics and nanofluidics* **2011**, *10*, 29-35.

(135) Rappaport, S. M.; Li, H.; Grigoryan, H.; Funk, W. E.; Williams, E. R. *Toxicology letters* **2012**, *213*, 83-90.

(136) Whitesides, G.; Stroock, A. *Phys Today* **2001**, *54*, 42-48.

(137) Batchelor, G. K. *An introduction to fluid dynamics*; Cambridge university press, 2000.

(138) Holmes, D. P., 2016.

(139) Hessel, V.; Löwe, H.; Schönfeld, F. *Chemical Engineering Science* **2005**, *60*, 2479-2501.

(140) Phelan, F. R.; Hughes, N. R.; Pathak, J. A. *Physics of Fluids* **2008**, *20*, 023101.

(141) Xu, N.; Lin, Y.; Hofstadler, S. A.; Matson, D.; Call, C. J.; Smith, R. D. *Analytical chemistry* **1998**, *70*, 3553-3556.

(142) Xiang, F.; Lin, Y.; Wen, J.; Matson, D. W.; Smith, R. D. *Analytical chemistry* **1999**, *71*, 1485-1490.

(143) Benetton, S.; Kameoka, J.; Tan, A.; Wachs, T.; Craighead, H.; Henion, J. D. *Analytical Chemistry* **2003**, *75*, 6430-6436.

(144) He, Y.; Wu, Y.; Fu, J.-Z.; Wu, W.-B. *RSC Advances* **2015**, *5*, 78109-78127.

(145) Kalish, B.; Tsutsui, H. *JoVE (Journal of Visualized Experiments)* **2016**, e53805-e53805.

(146) Ho, C. M. B.; Ng, S. H.; Li, K. H. H.; Yoon, Y.-J. *Lab on a Chip* **2015**, *15*, 3627-3637.

(147) Comina, G.; Suska, A.; Filippini, D. *Lab on a Chip* **2014**, *14*, 424-430.

(148) Naito, T.; Nakamura, M.; Kaji, N.; Kubo, T.; Baba, Y.; Otsuka, K. *Micromachines* **2016**, *7*, 82.

(149) Martinez, A. W.; Phillips, S. T.; Whitesides, G. M. *Proceedings of the National Academy of Sciences* **2008**, *105*, 19606-19611.

(150) Liu, H.; Crooks, R. M. *Journal of the American Chemical Society* **2011**, *133*, 17564-17566.

(151) Jang, I.; Song, S. *Lab on a Chip* **2015**, *15*, 3405-3412.

(152) Martinez, A. W.; Phillips, S. T.; Nie, Z.; Cheng, C.-M.; Carrilho, E.; Wiley, B. J.; Whitesides, G. M. *Lab on a Chip* **2010**, *10*, 2499-2504.

(153) Cao, Y.; Bontrager-Singer, J.; Zhu, L. *Journal of Micromechanics and Microengineering* **2015**, *25*, 065005.

(154) Wegmans, 2016.

(155) Foundation, G. C., 2016.

(156) Kucka, M.; Pogrmic-Majkic, K.; Fa, S.; Stojilkovic, S. S.; Kovacevic, R. *Toxicology and applied pharmacology* **2012**, *265*, 19-26.

(157) Mengel, D. B.; Purdue University Cooperative Extension Service.

(158) Noh, H.; Phillips, S. T. *Analytical chemistry* **2010**, *82*, 4181-4187.

(159) Tontisirin, K.; Nantel, G.; Bhattacharjee, L. *Proceedings of the Nutrition Society* **2002**, *61*, 243-250.

(160) Sarwar, M. *International Journal of Bioinformatics and Biomedical Engineering* **2015**, *1*, 130-136.

(161) Hamaguchi, N.; Ellington, A.; Stanton, M. *Analytical Biochemistry* **2001**, *294*, 126-131.

(162) Williams, R. M.; Crihfield, C. L.; Gattu, S.; Holland, L. A.; Sooter, L. J. *International journal of molecular sciences* **2014**, *15*, 14332-14347.

(163) Yan, J.; Yan, M.; Ge, L.; Yu, J.; Ge, S.; Huang, J. *Chemical Communications* **2013**, *49*, 1383-1385.

(164) He, M.; Li, Z.; Ge, Y.; Liu, Z. *Analytical chemistry* **2016**.

(165) He, M.; Liu, Z. *Analytical chemistry* **2013**, *85*, 11691-11694.

(166) Liu, Q.; Feng, W.; Yang, T.; Yi, T.; Li, F. *Nature protocols* **2013**, *8*, 2033-2044.

(167) Tennico, Y. H.; Hutanu, D.; Koesdjojo, M. T.; Bartel, C. M.; Remcho, V. T. *Analytical chemistry* **2010**, *82*, 5591-5597.

(168) Bagalkot, V.; Zhang, L.; Levy-Nissenbaum, E.; Jon, S.; Kantoff, P. W.; Langer, R.; Farokhzad, O. C. *Nano Letters* **2007**, *7*, 3065-3070.

(169) Behets, F.; Kashamuka, M.; Pappaioanou, M.; Green, T.; Ryder, R.; Batter, V.; George, J.; Hannon, W.; Quinn, T. *Journal of Clinical Microbiology* **1992**, *30*, 1179-1182.

(170) Randall, S. M.; Cardasis, H. L.; Muddiman, D. C. *Journal of the American Society for Mass Spectrometry* **2013**, *24*, 1501-1512.

(171) Fisher, R. A. **1935**.

(172) Porter, C. J.; Bereman, M. S. *Journal of Proteins & Proteomics* **2014**, *5*.

(173) Porter, C. J. **2015**.

APPENDICES

A.1 Design of Experiment Optimization

A.1.1 Introduction

Design of Experiment (DOE) was used to identify parameters which significantly affected the signal from paper spray ionization. DOE was pioneered by R. Fisher and has been utilized in a wide swath of mass spectrometry applications.[170-173] DOE has been used in both academia and industry to both study the effect of individual factors as well as interactions between multiple factors on output in an effort to save time and money. In paper spray ionization protocols and procedures, there are several factors which have the potential to provide increased sensitivity when optimized. DOE was used to optimize select experimental parameters, see **Table A.1**, and help create a standard experimental procedure for later experiments.

A.1.2 Materials and Methods

Materials

Rhodamine 6G dye (R6G) was obtained from Sigma-Aldrich (St. Louis, MO). High performance liquid chromatography (HPLC) grade methanol and water were from Burdick and Jackson (Muskegon, MI). Whatman Grade 1 and 2 filter paper sheets of were purchased from GE Healthcare Bio-Sciences (Pittsburgh, PA). All mass analyses were performed using a LTQ Ion Trap mass spectrometer (Thermo Scientific, Bremen, Germany).

DOE on Paper Spray Parameters

Design Expert software version 9.0.3.1 (Stat-Ease inc. Minneapolis, MN) was used to design the paper spray optimization DOE experiment. The experimental design had a

resolution of 4 allowing for main effects and 2nd order interactions to be determined which resulted in 16 conditions to analyze 8 factors. The factors and levels tested were: applied voltage (2, 4kV), capillary temperature (250, 350 ^{o}C), paper treatment (unwashed, washed), tip creation (cut, folded), dry time (0, 1 hr), paper type (Whatman 1, Whatman 2), tube lens voltage (60, 150 V), and solvent composition (50% Methanol, 50% Acetonitrile).

Experimental Procedure

A piece of either washed or unwashed Whatman 1 or Whatman 2 filter paper was either folded into a triangle or a cut into a triangle and loaded with a 10µl aliquot of 100µM R6G dye solution. The loaded piece of paper was either tested immediately after sample loading or allowed to dry for one hour. 50 µl of a 1:1 solution of either MeOH:H_2O or Acetonitrile:H_2O was loaded on to the paper. The paper triangle was positioned in front of the mass spectrometry and a voltage of either 2 or 4 kV was applied. The LTQ ion trap's capillary temperature was set to either 250 or 350 ^{o}C and tube lens voltage was set to either 60 or 150 V, depending on each particular runs testing parameters. The parent R6G dye ion (*m/z* 445) was isolated and fragmented. The primary transition's signal (*m/z* 415) was recorded. Analysis was taken for one minute for all samples.

A.1.3 Results and Discussion

Table A.1 summarizes the parameters selected for optimization and motivation for examining each factor. Some parameters selected for exploration are commonly used paper spray parameters from the literature: applied voltage, tip creation, and capillary temperature.

Other parameters were chosen for exploratory reasons: paper treatment, paper type, and solvent composition.

Table A.1: Parameters selected for optimization and their motivations.

Parameters(Levels)	Motivation
Applied Voltage (2 , 4 kV)	**Is a "low" or "high" voltage needed for spray initiation?**
Capillary Temperature (250 , 350 ºC)	**Does inlet temperature affect signal?**
Paper Treatment (Unwashed , Washed)	**Does washing the paper beforehand with the spray solvent increase signal?**
Tip Creation (Cut , Folded)	**Does the spray tip need to be sharp?**
Dry Time (0 , 1 hr)	**Does allowing the analyte to dry increase signal?**
Paper Type (Whatman 1 , Whatman2)	**Do different papers give different responses?**
Tube Lens Voltage (60 , 150 V)	**Does counter electrode voltage strength affect signal?**
Solvent Composition (50% Methanol , 50% Acetonitrile)	**Does the volatile organic in spray solvent matter?**

Figure A.1 shows the half-normal plot for the model with all selected parameters labels. Parameters that had high standardized effects, parameters on the far right of the graph, and parameters far off the trend line were also selected in the model's evaluation. The Capillary Temperature parameter was also included due to aliasing.

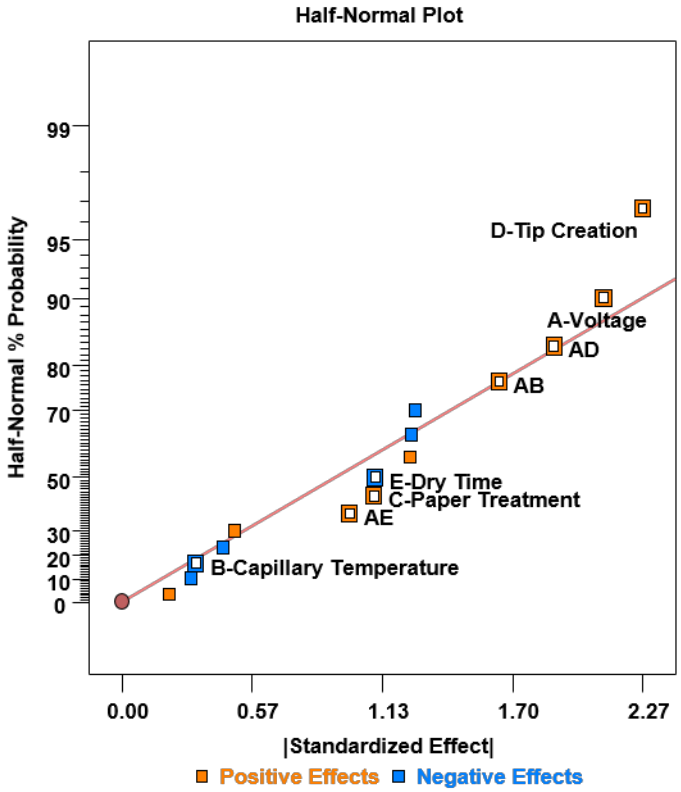

Figure A.1: Half-Normal plot used in evaluating the significance of factors during DOE optimization. Factors included in the systems analysis are highlighted and labels

Table A.2 summarizes the results obtained from analysis of the paper spray optimization parameters through DOE. The output measured was the peak area of the R6G fragment ion (*m/z* 415). Peak areas were extracted from Thermo Fisher Xcalibur and values were inputted into Design Experiment. Parameter p-values were calculated by analysis of variance (ANOVA) with an alpha value of 0.05. The higher applied voltage, 4 kV, was found to be significant ($p < 0.05$). This was expected as this setting is a standard in the literature. Another literature standard that was found to be significant was the “Cut” form of tip creation. The remaining parameters included in the model’s analysis were all found to be non-significant

($p > 0.05$). These results were not unexpected as both levels of each of these parameters can be found in the literature. Therefore, either level could be used without significant change in detection.

Table A.2: Summary of results from the optimization with MS2 peak area as the measured output. Only parameters used in the model's evaluation are included. Favorable conditions in significant parameters ($p < 0.05$) are underlined.

Parameters(Levels)	P-Value
Applied Voltage (2 , <u>4</u> kV)	**0.0479**
Capillary Temperature (250 , 350ºC)	**.7232**
Paper Treatment (Unwashed , Washed)	**0.2504**
Tip Creation (<u>Cut</u> , Folded)	**0.0361**
Dry Time (0 , 1 hr)	**0.2484**

A.1.4 Conclusions

Herein, the optimization of paper spray ionization via DOE has been described. This experiment was performed before any other experiment described in this thesis in order to establish a baseline protocol. All significant levels were included in all aforementioned experiments as they are standards in the field: 4 kV applied voltage and cut tip creation. Although slight changes would be made during later experiments, these results would represent the base protocol.

A.2 3D Printed Cartridge

A.2.1 Introduction

3-dimensional (3D) printed cartridges have been used in conjunction with paper spray mass spectrometry for several years[39,40,98]. These devices have predominantly provided structural support to the rather flimsy paper substrate but also have been designed to incorporate other functionalities. These functionalities have included continuous solvent application[40] and the integration of pretreatment devices, such as solid phase extraction[39]. In attempts to increase our paper spray substrate's structural integrity and add the capacity for later on-device functionalization, a simple 3D cartridge was printed to test for solvent capability and serve as a base model for later functionalizations.

A.2.2 Materials and Methods

Materials

High performance liquid chromatography (HPLC) grade methanol and water were purchased from Burdick and Jackson (Muskegon, MI).

Fabrication of 3D Device

A simple 3D cartridge was designed using a browser based 3D modeling program called Tinkercad by Autodesk. An image of the 3D rendering of both the top and bottom segments can been seen in **Supplemental Figure A.2** and a labeled image of the bottom segment can be seen in **Supplemental Figure A.3**. The cartridge was printed at the North Carolina State University's Hunt Library Makerspace on a Fusion3 F306 Gen 1 3D Printer. The printer's resolution was set to .2mm and the output density was set to medium. All other

factory settings were left unaltered. A final product image with can been seen in **Supplemental Figure A.4**. Polyactic acid (PLA) plant-based plastic was used to print the device. Three small cubes, 2 cm^3 total volume, of the PLA plastic were also printed, as to test for solvent capability without needlessly harming the whole device.

Solvent Capability

The three small cubes of PLA plastic were placed in separate beakers consisting of solutions with different percent methanol concentrations: 0%, 50%, or 100% respectively. The cubes were allowed to sit in the solution for three minutes, roughly the time for a full paper spray analysis to occur. After three minutes, the cubes were removed and their structural integrity was assessed.

A.2.3 Results and Conclusions

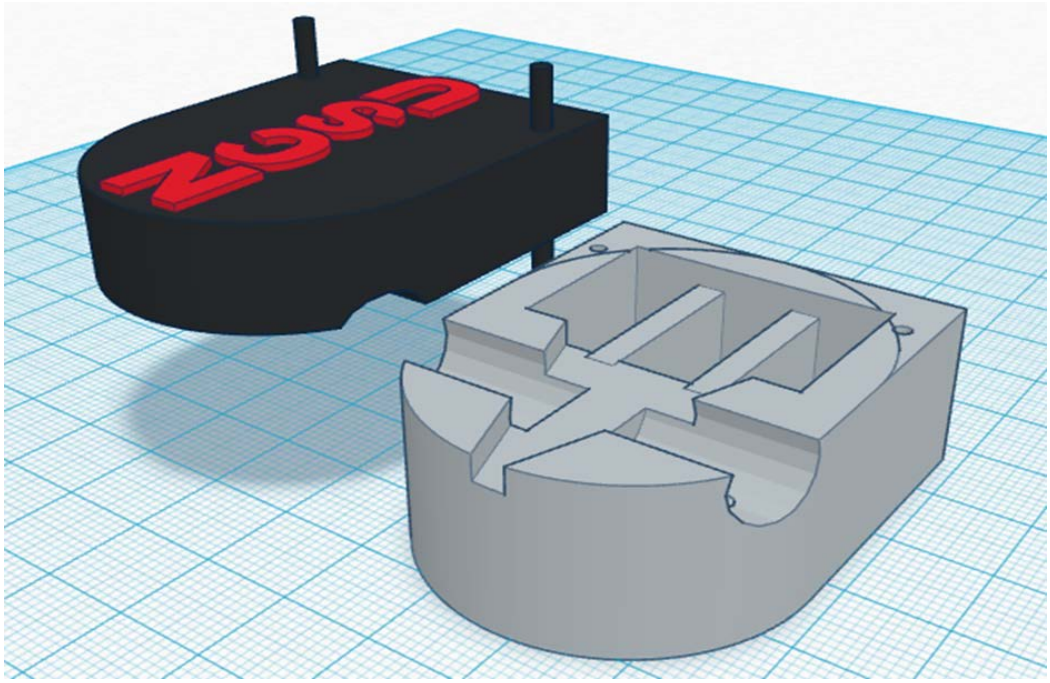

Figure A.2: Digital rendering of both the top and bottom segments of the 3D printed paper spray cartridge.

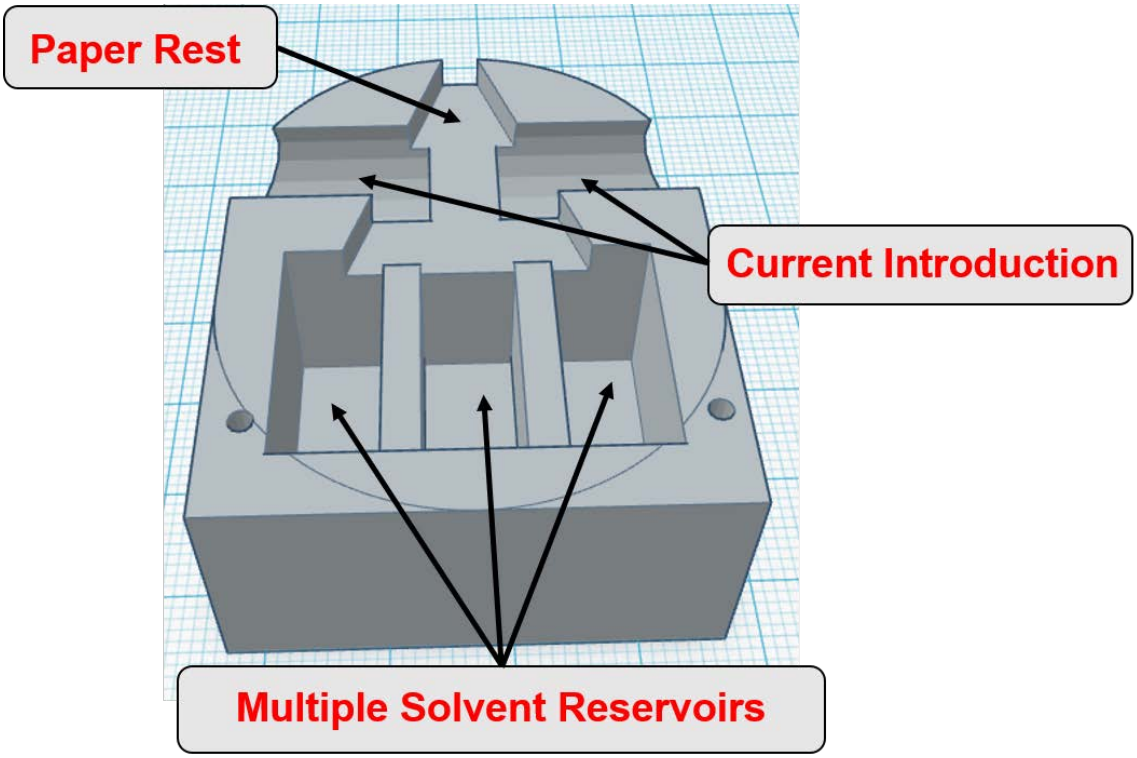

Figure A.3: Digital rendering of the bottom segment of the 3D printed paper spray cartridge, with important features labeled.

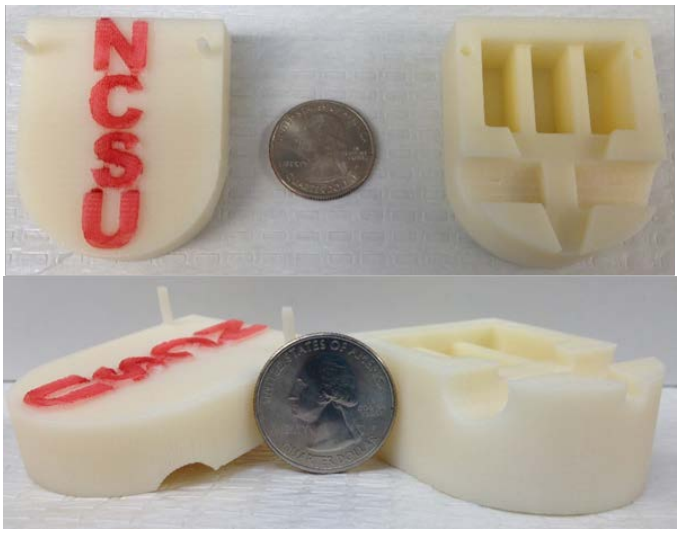

Figure A.4: **(Top)** Top down image of both halves of the 3D printed cartridge. **(Bottom)** Side view image of both halves of the 3D printed cartridge. A quarter is included for scale

After removal from the methanol solutions, the three cubes showed varying degrees of decreased structural integrity. The cube in 0% methanol showed no loss of structural integrity. It was as firm to light pressure as it was before solution exposure. In comparison, the cubes exposed to the 50% and 100% methanol solutions showed considerable loss of structural integrity. The cube in 50% methanol was fairly malleable under light pressure and the methanol solution had taken on a very light murkiness, similar in tint to the plastic itself. The cube in 100% methanol was vary malleable, almost to the point of complete dissolution if handled with any force. The solution had taken on a cloudy appearance, similar in tint to the plastic itself.

These results demonstrate an incompatibility with methanol solutions, a commonly used paper spray solvent. While other commonly used paper spray solvents such as acetonitrile were not tested, it was assumed that other organics would have similar results. Compatible plastics have been referenced in the literature[40,98,146] but local printing services did not offer these materials. Also, custom ordering proved to be cost prohibitive and counter to our intent of rapid creation and customization. Therefore, due to this solvent incompatibility and lack other cost-effective printing options, including both plastic material and printing facilities, further work in creating a 3D cartridge was halted.

A.3 Supplemental Designs

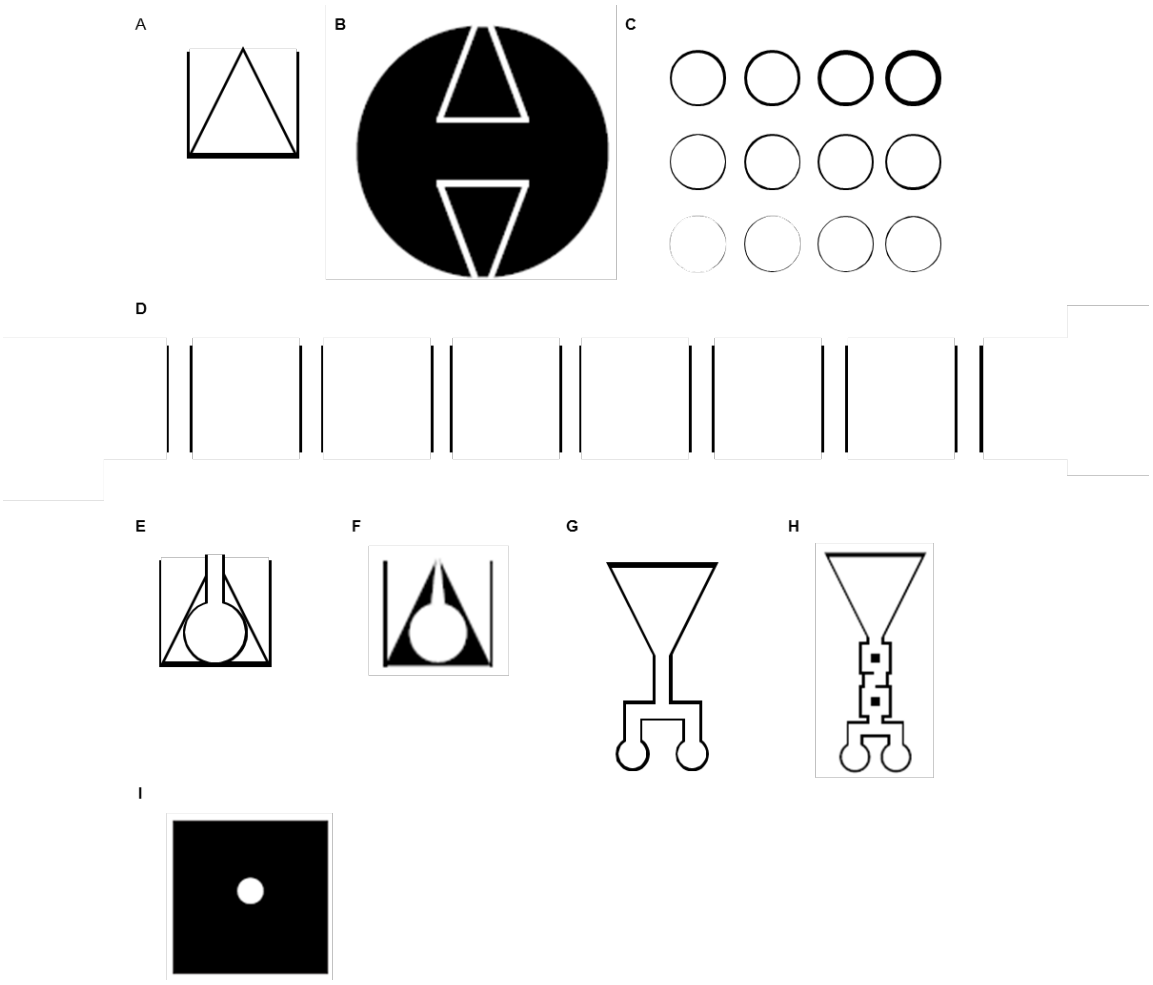

Figure A.5: All designs used during the experiment. Designs were created in Adobe Illustrator and exported as PDF's for use. **(A)** Simple wax barrier design. **(B)** Photoresist mask design. Printed on transparency by DTPRESS Commercial Printing (Greensboro, NC). **(C)** 12 wax-printed wells varying from 1mm to .05mm in width. Latter wells might appear non-existent in print due common printer limitations. **(D)** Seven sets of equivalent wax parallel lines used to determine wall swelling from organics. Only 6 were used during the experiment. **(E)** Constricted wax design. **(F)** Increasingly restricted wax design. **(G)** Wax mixing design **(H)** Variable channel width wax mixing design also called chaotic advection design. **(I)** Single layer used in 3D devices.

Acknowledgements

I would like to acknowledge NC State University for Startup funds. I would also like to acknowledge the use of the Analytical Instrumentation Facility (AIF) at North Carolina State University, which is supported by the State of North Carolina and the National Science Foundation.